Carbon dioxide cycling through the mantle and implications for the climate of ancient Earth

Kevin Zahnle and Norman H. Sleep

Email alerting service	click here to receive free e-mail alerts when new articles cite this article
Permission request	click here to seek permission to re-use all or part of this article
Subscribe	click here to subscribe to Geological Society, London, Special Publications or the Lyell Collection

Notes

Lyell
Collection

Carbon dioxide cycling through the mantle and implications for the climate of ancient Earth

KEVIN ZAHNLE[1] & NORMAN H. SLEEP[2]

[1] *NASA Ames Research Center, Mountain View, CA 94035, USA*
(e-mail: kzahnle@mail.arc.nasa.gov)
[2] *Department of Geophysics, Stanford University, Stanford, CA 94305, USA*

Abstract: The continental cycle of silicate weathering and metamorphism dynamically buffers atmospheric CO_2 and climate. Feedback is provided by the temperature dependence of silicate weathering. Here we argue that hydrothermal alteration of oceanic basalts also dynamically buffers CO_2. The oceanic cycle is linked to the mantle via subduction of carbonatized basalts and degassing of CO_2 at the mid-ocean ridges. Feedback is provided by the dependence of carbonatization on the amount of dissolved carbonate in sea water. Unlike the continental cycle, the oceanic cycle has no thermostat. Hence surface temperatures can become very low if CO_2 is the only greenhouse gas apart from water. Currently the continental cycle is more important, but early in Earth's history the oceanic cycle was probably dominant. We argue that CO_2 greenhouses thick enough to defeat the faint early Sun are implausible and that, if no other greenhouse gases are invoked, very cold climates are expected for much of Proterozoic and Archaean time. We echo current fashion and favour biogenic methane as the chief supplement to CO_2. Fast weathering and probable subduction of abundant impact ejecta would have reduced CO_2 levels still further in Hadean time. Despite its name, the Hadean Eon might have been the coldest era in the history of the Earth.

Introduction

Evidence for relatively mild climates on ancient Earth has been a puzzle in light of the faint early Sun (Ringwood 1961; Sagan & Mullen 1972; Kiehl & Dickinson 1987; Pavlov *et al.* 2000). The usual solution has been to posit massive CO_2 atmospheres (Owen *et al.* 1979; Kasting 1993), although reduced gases (e.g. NH_3 or CH_4) have had their partisans (Sagan & Mullen 1972; Pavlov *et al.* 2002). Evidence against siderite in palaeosols has been used to set a rough upper limit of 30 PAL (present atmospheric levels, where one PAL = 300 ppm) on pCO_2 *c.* 2.75 Ga (Rye *et al.* 1995), which is less than what is needed to defeat the faint Sun (Rye *et al.* 1995). We present here an independent argument, based on CO_2 fluxes into and out of the mantle, that weighs against high pCO_2 on early Earth, especially during the Archaean and Hadean eons.

There are roughly 5×10^{21} moles of carbon in the crust and more in the mantle (e.g. Zhang & Zindler 1993; Wedepohl 1995). The current CO_2 mantle outgassing rate at the mid-ocean ridges, $(1.5-2.5) \times 10^{21}$ mol a^{-1} (Marty & Jambon 1987), is fast enough to double the crustal inventory in 2–3 Ga. Greater heat flow on early Earth implies faster outgassing, probably reducing the doubling time for crustal carbon to < 1 Ga in Archaean time. The large source implies a large

sink to close the mantle cycle. Possibilities include subduction of carbon directly deposited on the ocean floor (pelagic carbonates and organic carbon); subduction of carbon that is scraped off continents and dragged down; and subduction of carbonates formed by sea-water alteration of the oceanic basalt itself. The last depends on the amount of free CO_2 in the ocean, and hence can act as a buffer on atmospheric CO_2 levels.

Here we construct a specific albeit extremely simplified model of the modern CO_2 cycle. We then accelerate the cycle into Archaean time. Then we consider the effects of abundant impact ejecta on the Hadean CO_2 cycle. Throughout we neglect the sometimes different behaviour of reduced carbon, as terms involving reduced carbon are relatively small and the complications and uncertainties introduced by modelling of the oxygen cycle relatively large. This precludes our using carbon isotopes to constrain our models. This paper is intended as an abbreviated and updated version of Sleep & Zahnle (2001). The focus of this paper is on a simpler presentation of model results, although we also clarify the relative insensitivity of our results to the seafloor spreading rate; the earlier paper placed undue emphasis on this factor. We defer to the earlier paper for detailed discussions of the geological data and weathering rates. We also use this opportunity to correct a typographical error

that eventually propagated through the earlier paper's discussion of the volume and weathering of impact ejecta during Hadean time.

The current carbonate cycle

On geological time scales, CO_2 cycles between rocks, often by way of the ocean and atmosphere. The rock reservoirs include the mantle, continental carbonates, carbon in reduced form mostly in continental shales, and carbon (mostly carbonate) in or on the sea floor. The small volatile reservoir (ocean plus atmosphere) cycles through carbonate rock in a hundred thousand to a million years. Over longer periods free CO_2 is dynamically controlled by processes that form carbonates at low temperatures and processes that decompose carbonates at high temperatures by (Urey) reactions of the form

$$CO_2 + CaSiO_3 \Leftrightarrow SiO_2 + CaCO_3. \quad (1)$$

Magnesium and, under reducing conditions, iron carbonates can form by analogous reactions. The continental part of this cycle has been extensively studied (e.g. Walker 1977; Holland 1978, 1984; Franck *et al.* 1999). Weathering of rocks on land dissolves carbonates and releases Ca^{2+} from silicates. Both the dissolved carbonate and calcium are carried by rivers to the oceans, where they react to form $CaCO_3$. Reaction (1) is reversed when carbonates are metamorphosed deep in the crust. Carbonate weathering,

$$H_2O + CO_2 + CaCO_3 \Leftrightarrow Ca^{2+} + 2HCO_3^- \quad (2)$$
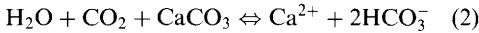
is usually regarded as having no direct net effect on carbonate reservoirs on time scales longer than a few thousand years, but silicate weathering, by removing free CO_2 from the atmosphere–ocean system, acts to buffer surface temperatures, because the weathering rate increases with temperature, and temperature rises with atmospheric CO_2 (Walker *et al.* 1981; Lasaga *et al.* 1985).

We follow Tajika & Matsui (1992) and apportion carbonate between five significant reservoirs: the atmosphere and ocean, R_{oc}; carbonates lying upon (R_{pel}) or veined within (R_{bas}) oceanic basalt; carbonates on continental platforms, R_{con}; and CO_2 in the mantle, R_{man}. The atmosphere and ocean are tightly coupled on geological time scales. We treat these together as a single reservoir with a current size of c. 3.3×10^{18} moles.

The budget for R_{oc} can be written as

$$\frac{\partial R_{oc}}{\partial t} = F_{meta} + F_{ridge} + F_{arc} + F_{CO_3w}$$
$$- F_{dep} - F_{pel} - F_{SiO_3w} - F_{hydro} - F_{ej}. \quad (3)$$

Sources are the metamorphic flux (F_{meta}), outgassing at mid-ocean ridges (F_{ridge}), outgassing associated with arc volcanoes (F_{arc}), and carbonate weathering (F_{CO_3w}). Sinks are carbonate deposition (F_{dep}) on continental platforms, pelagic carbonate deposition on oceanic crust (F_{pel}), silicate weathering on continents (F_{SiO_3w}), carbonatization of oceanic crust in warm hydrothermal systems (F_{hydro}), and carbonatization of impact ejecta (F_{ej}), respectively. The last is restricted to Hadean time.

The carbonate budget for the oceanic crust $R_{bas} + R_{pel}$ can be written as

$$\frac{\partial(R_{bas} + R_{pel})}{\partial t} = F_{pel} + F_{tect} + F_{hydro}$$
$$+ F_{ej} - F_{sub} - F_{scrape}. \quad (4)$$

Pelagic carbonates, tectonic erosion (F_{tect}, carbonate swept up by the oceanic crust just before subduction), and hydrothermal and ejecta carbonatization add to the inventory of carbonate on or in the oceanic crust. Losses are subduction (F_{sub}) and 'off-scraping' (F_{scrape}, carbonate removed from the oceanic crust just before subduction). By presumption, the subduction flux F_{sub} is proportional to what is on or in the sea floor ($R_{pel} + R_{bas}$), and both F_{sub} and F_{scrape} are inversely proportional to the lifetime of the oceanic crust. The relative importance of subduction and off-scraping depends on whether the carbonate sits on or within the oceanic crust. For example, pelagic carbonates will be more easily scraped off than would carbonatized basalt. In addition to these terms, significant amounts of continentally derived sediments and crust tectonically eroded by the slab are also subducted. We have lumped these together as F_{tect} and accounted them separately from F_{sub}. Neither F_{tect} nor F_{scrape} are well constrained. For modelling purposes we make the arbitrary assumption that the tectonic terms are equal and opposite, so that $F_{tect} = F_{scrape}$.

The continental and mantle budgets are then written as

$$\frac{\partial R_{con}}{\partial t} = F_{SiO_3w} + F_{dep} - F_{CO_3w} - F_{meta} \quad (5)$$

and

$$\frac{\partial R_{man}}{\partial t} = C_{deep}F_{sub} - F_{ridge} \quad (6)$$

respectively. Both reservoirs are large. Representative estimates of their current sizes are $R_{con} = 4 \times 10^{21}$ moles and $R_{man} = (11–18) \times 10^{21}$ moles. At present R_{con} is shrinking because of pelagic carbonate deposition; there are roughly $R_{pel} = 1 \times 10^{21}$ moles of pelagic carbon on the sea floor

that have been recently removed from the continents (Wilkinson & Walker 1989). A fraction C_{deep} of the total subduction flux F_{sub} reaches the deep mantle, whereas the balance $(1 - C_{deep})F_{sub} = F_{arc}$ is shunted through arc volcanoes. We think that C_{deep} is not small: we estimate that it is currently $c.75\%$ (see below), so that only about a quarter of the subducted carbon fails to reach the mantle.

Continents

The largest fluxes in equations (3)–(6) are those associated with carbonate weathering, which consumes and redeposits carbonates at a rate of $c.2 \times 10^{13}$ moles a^{-1}. The associated time scales for recycling R_{con} and R_{oc} are 3×10^8 and 2×10^5 a, respectively. It is sometimes argued that, because carbonate weathering liberates both the anion and the cation (e.g. Ca^{2+}), it serves merely to move calcium carbonate from place to place with no net effect on R_{oc} or the overall carbonate budget. For simplicity we will accept this argument. But at present carbonate weathering and pelagic deposition are moving carbonate from the continents to the sea floor, so that $F_{CO_3w} \approx F_{dep} + F_{pel}$. Thus carbonate weathering currently acts as a net sink on continental carbonate, and to the extent that pelagic carbonate is or will be subducted, it will constitute a net loss of crustal carbonate.

Pelagic carbonates accumulate where the $CaCO_3$ shells made by planktonic organisms fail to dissolve before they reach the ocean floor. Currently F_{pel} is rather large. Catubig et al. (1998) estimated that $F_{pel} \approx (8-9) \times 10^{12}$ moles a^{-1}. But such planktonic organisms precipitated insignificant amounts of carbonate before the middle of Mesozoic time (Sibley & Vogel 1976) and little pelagic $CaCO_3$ is now being subducted compared with the amount being deposited on the sea floor (Plank & Langmuir 1998). When extrapolating the CO_2 cycle into the distant past we set F_{pel} to zero and $F_{CO_3w} = F_{dep}$.

The metamorphic and silicate weathering fluxes are somewhat smaller. Combined, the arc volcanic and metamorphic fluxes are estimated at $(6-6.8) \times 10^{12}$ moles a^{-1} (Brantley & Koepenick 1995; Goddéris & François 1995). Most of this is metamorphic. At current rates the continental carbon inventory is recycled over some 600–800 Ma. For modelling purposes it is usually assumed that silicate weathering and metamorphism balance over time scales of hundreds of millions of years. We will begin our analysis with this case, in which fluxes in and out of the mantle are ignored, to establish context for models that include the mantle.

With the above simplifications equation (3) reduces to an implicit equation for the steady-state value of R_{oc}:

$$F_{SiO_3w} + F_{hydro} + F_{ej} = F_{meta} + F_{ridge} + F_{arc}.$$
(7)

In equation (7), the fluxes on the left-hand side are all monotonically increasing functions of R_{oc} (or pCO_2), whereas the terms on the right-hand side are independent of R_{oc}.

Silicate weathering is a strong function of temperature T and a weak function of pCO_2. For simplicity we follow *Walker et al.* (1981) and use

$$F_{SiO_3w} = C_{SiO_3w}pCO_2^\beta \exp[(T - T_0)/B]$$
(8)

where $B = 13.7$ and $\beta = 0.3$ are the weathering parameters suggested by Walker et al. (1981), and C_{SiO_3w} and T_0 are calibration constants.

To obtain pCO_2 histories we need to specify histories of metamorphic recycling and solar luminosity, and we need to parameterize the greenhouse effect. We relate the metamorphic flux to the size of the continental reservoir, $F_{meta} = R_{con}/\tau_{meta}$, where τ_{meta} is the time scale over which continental carbonate is metamorphosed. We assume that the rate of carbonate metamorphism is proportional to the global heat flow Q. We take Q to decrease as $(1 - t/4.5)^\mu$ with $\mu = 0.7$ for high heat-flow models and $\mu = 0.2$ for low heat-flow models. Solar luminosity increases as $L = L_0(1 - 0.07t)$. In both these expressions the time t is in Ga. The heat-flow function is arbitrary; the solar luminosity evolution standard. We use Caldeira & Kasting's (1992) parameterization of the CO_2–water vapour greenhouse effect with an albedo of 31% (so as to reproduce current pCO_2 and T_0). The ice–albedo feedback, which predicts that global ice cover would amplify global cooling, is ignored. Studies of palaeosols constrain pCO_2 in the past 400 Ma to between 1 and 10 PAL (Ekart et al. 1999). We calibrate silicate weathering by assuming a long-term average pCO_2 level of 3.0 PAL and $T_0 = 290$ K.

Illustrative temperature and pCO_2 histories obtained solving equation (8) are shown in Figure 1 for two values of β and (for comparison) for constant pCO_2. The Urey buffer working alone predicts clement ancient climates only if silicate weathering is a weak function ($\beta < 0.2$) of pCO_2. Two observations pertinent to any successful CO_2 climate buffer are that (1) it takes a lot of CO_2 to maintain clement climates and (2) the predicted climates are not necessarily particularly clement. They are usually cooler than
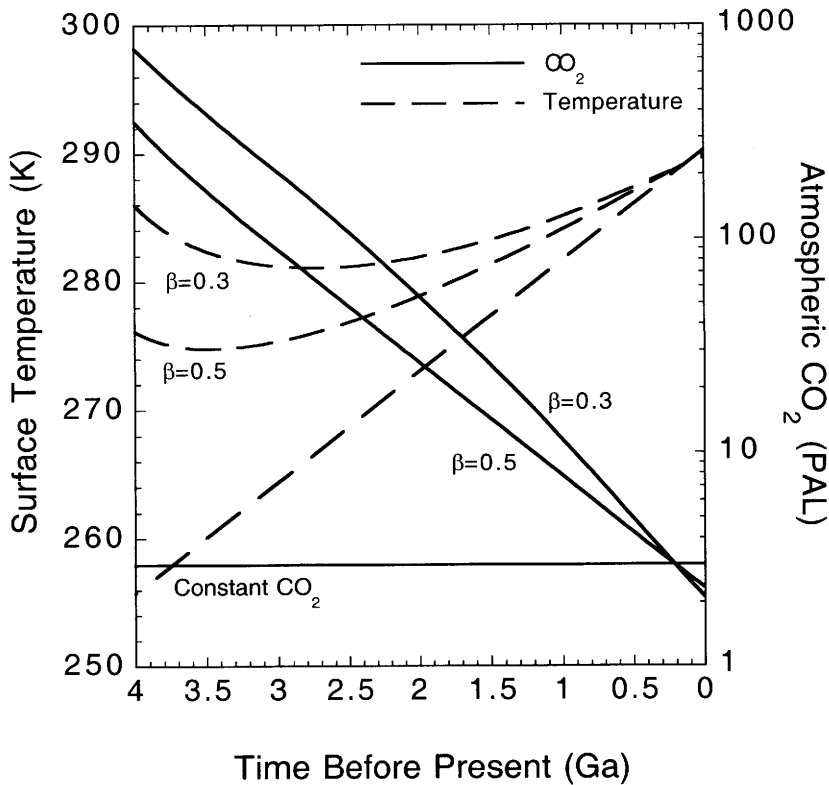
K. ZAHNLE & N. H. SLEEP

Fig. 1. Global average surface temperatures and atmospheric CO_2 levels predicted by models in which CO_2 is the only greenhouse gas and the temperature dependence of subaerial silicate weathering is the only effective buffer against changing solar luminosity. One PAL indicates one 'present atmospheric level' of 300 ppm. Curves are labelled by the weathering parameter β (equation (8)). These models are inspired by Walker *et al.* (1981). Constant CO_2 is shown for comparison. Unless silicate weathering is nearly independent of pCO_2 ($\beta < 0.2$), ancient climates are cool.

the modern climate through most of Precambrian time. An additional effect is required if warmer Precambrian climates are desired. The best explored of these is a hypothesized biotic enhancement of weathering.

Biotic enhancement of weathering means that plants (via roots, respiration and humic acids) increase the effective reaction rate (C_{SiO_3w} in equation (8)) of atmospheric CO_2 with silicates. This can be important if it changes over time. Schwartzman & Volk (1989, 1991) appeared to argue implicitly that C_{SiO_3w} has grown monotonically as the biota became ever better at extracting minerals from the Earth. Their argument is slightly Gaian if it is used to maintain a temperate climate, because it implies that the evolution of biotic weathering has tracked the evolution of the Sun. In later work Schwartzman & McMenamin (1993) went beyond Gaia and argued that biotic weathering has evolved

faster, and that despite the brightening Sun, Earth's climate has systematically cooled (the current enhancement in C_{SiO_3w} over that before life would be of order 1000). Schwartzman emphasized the importance of plants stabilizing soils as a means of speeding chemical erosion. This can be questioned. The soils serve not just as micro-environments that might promote chemical weathering but also as armour that can protect the underlying rock. It is not obvious which effect is, on global average, the more important.

Berner (1994, 1997) also emphasized biotic weathering. In his model the advent of vascular land plants and their root systems leads to a step function change in the biotic weathering enhancement beginning in Devonian time. Berner (1994) used more complicated expressions for silicate weathering than we do. These explicitly include topography, runoff, vegetation and

climate feedback. When cast in the form of equation (8), Berner's choices are equivalent to taking $B = 11.1$ and $\beta = 0.5$, the latter pertinent before the advent of vascular land plants. Beginning with Devonian time, Berner regarded silicate weathering as dependent on elevated concentrations of CO_2 in the soil: for a given pCO_2, weathering goes some 3–10 times faster with roots than without roots (Berner 1997), but is nearly independent of pCO_2 (roughly equivalent to $\beta \approx 0.14$). Berner relied heavily on data obtained from weathering of recent tillites and recent volcanic rocks. Whether his arguments are appropriate for old soils such as tropical laterites is an open question. To quantify the possible effect of plant roots, we compute 'roots' models (the dotted curves in Fig. 2). In these models we reduce the weathering rate before the advent of roots to 30% of the current rate. For consistency with Berner we use $\beta = 0.5$. The rooted models are especially warm at the end

of Precambrian time (see Berner 1997), which may make them a poor match to the climate of the time.

Another factor that can influence the weathering rate is the subaerial extent of the continents. Schwartzman included continental area as a multiplicative factor in his expression for the weathering rate. We think this factor has been overstated. It has been argued that continents grew slowly and only reached their present mass at $c.\,2\,Ga$. This view is not universal, and if anything the arguments for constant continental volume seem currently the stronger (Bowring & Housh 1995; Wilde et al. 2001; Mojzcis et al. 2001). Yet if we suppose the continents to have been much smaller in Archaean time, we need also suppose that the continental volcanic and metamorphic CO_2 fluxes were proportionately smaller in Archaean time. The volcanic source cannot simply be held constant while the weatherable surface is shrunk to insignificance.
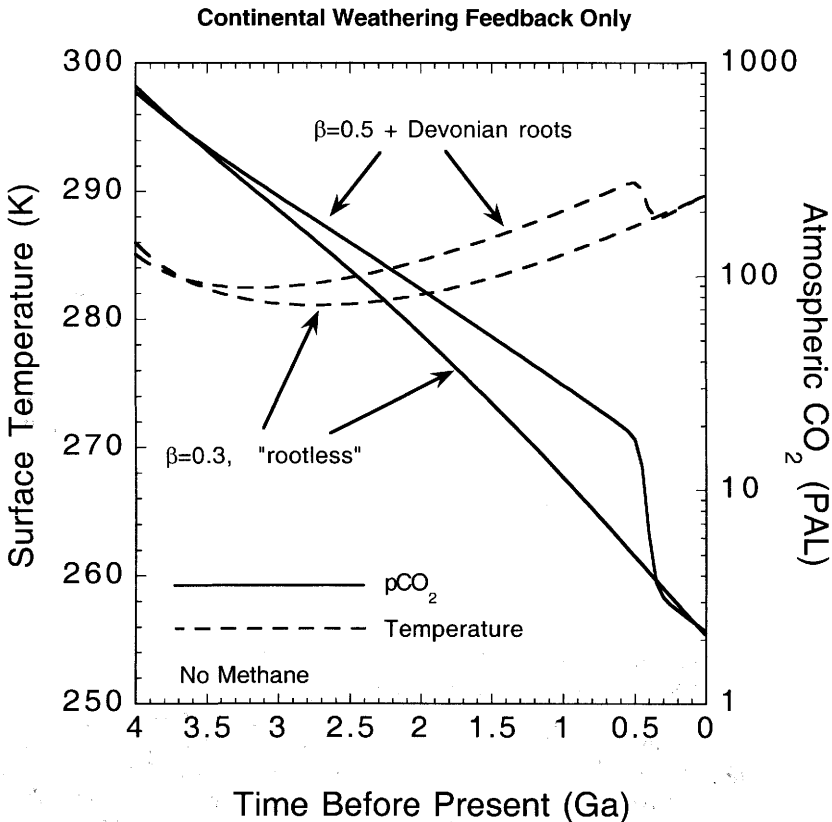
Continental Weathering Feedback Only

Fig. 2. Comparison of continent-only models with and without an abrupt change in weathering efficiency caused by the advent of vascular land plants in Devonian time. The 'Devonian roots' model uses parameters that follow Berner (1994) as much as possible.

Shrinking the continents reduces their importance as a source as well as a sink of CO_2 *vis à vis* the sea floor.

The fainter Archaean Sun presents a greater challenge. A warm Archaean climate demands 100–1000 PAL CO_2. Such high CO_2 levels appear to conflict with the absence of siderite in 2.75 Ga palaeosols (Rye *et al.* 1995; see Figure 7 below). They also imply that ancient oceans were much depleted in Ca^{2+}. The resulting CO_2-rich, Ca-poor sea water would have been much more effective than modern waters at leaching Ca from basalts and much more prone to carbonatize basalts *in situ*. Extreme Ca depletion of ancient seawaters would seem to be inconsistent with evidence for evaporitic gypsum (Buick & Dunlop 1990).

The mantle

As discussed in the Introduction, CO_2 exchange with the mantle becomes important on Earth's longest time scales. We consider in detail two sources (arc volcanoes and the mid-ocean ridge) and one sink (subduction of carbonitized basalts).

Arc volcanism

Arc volcanism and subduction are related, with arc volcanoes tapping subducted carbonate. We (Sleep & Zahnle 2001) estimated that $F_{arc} = 1.2 \times 10^{12}$ moles a^{-1}. Our estimate is revised downwards from that by Sano & Williams (1996): we assumed an arc volcanism rate of 2 km^3 a^{-1} that is consistent with estimates by Plank & Langmuir (1998), whereas Sano & Williams used 5 km^3 a^{-1}. Our estimate for F_{arc} is at the low end of the range estimated by Marty & Tolstikhin (1998); the difference appears to stem from their presuming higher rates of arc volcanism (8 km^3 a^{-1}) than we. F_{arc} is a significant fraction of the crustal metamorphic flux ($(6–6.8) \times 10^{12}$ moles a^{-1}) used in other models of the global CO_2 cycle (Brantley & Koepenick 1995; Goddéris & François 1995). Currently, about 75% of the carbon in F_{arc} comes from subducted carbonate, 1/8 from organic matter in subducted sediments, and 1/8 from normal mantle. These fractions imply that some hemipelagic sediments and tectonically eroded crust, which have organic matter as well as pelagic sediments, are subducted and then degassed. The fraction of CO_2 derived from carbonate does not correlate with locations where large amounts of sedimentary carbonate are being subducted (Plank & Langmuir 1998). This indicates that significant amounts of carbonate are within altered basalt as we discuss below. In a detailed study of Kudryavy volcano on the Kurile Islands, Fischer *et al.* (1998) found that 1/6 of the subducted carbonate and 1/3 of the subducted organic carbon are returned to the surface in arc magmas. We ignore the true mantle source at arc volcanoes as small compared with uncertainties in F_{ridge}.

To calibrate C_{deep}, we take the current flux of pelagic carbonate into subduction zones to be 1.4×10^{12} moles a^{-1}. This is the global extrapolation of the flux reported by Plank & Langmuir (1998). It is currently part of F_{sub}. We take $F'_{sub} = 3.4 \times 10^{12}$ mole a^{-1} as the flux of carbonatized oceanic crust currently entering subduction zones. The latter is Alt & Teagle's (1999) estimate based on carbonate in boreholes in oceanic crust. It is similar to Zhang & Zindler's (1993) estimate of 4×10^{12} moles a^{-1}, which is based on measurements of CO_2 (Staudigel *et al.* 1989, 1996) in older crust formed at fast ridges in the Pacific that is about to be subducted. Leaving subduction zones we have $F_{arc} = 1.2 \times 10^{12}$ moles a^{-1}. As discussed above, we assume $F_{tect} = F_{scrape}$. This leaves $C_{deep} = 75\%$, consistent with the direct estimate from a Kurile arc volcano of 64–84% (Fischer *et al.* 1998). High values of C_{deep} are consistent with the thermodynamic stability of carbonates under experimental conditions that simulate those encountered during subduction (Kerrick & Connolly 2001). These experiments indicate that carbonates should mostly survive subduction under most regimes, present or past. In any case, low values of C_{deep} are problematic, as they would imply that CO_2 cannot return to the mantle. The problem would be worse in the past when the mantle was warmer and C_{deep} smaller. If C_{deep} becomes too small then CO_2 is stranded at the surface. When the amount of CO_2 at the surface exceeds the available pool of accessible cations the CO_2 builds up in the atmosphere and the climate becomes insufferably hot. These matters have been discussed in more detail elsewhere (Sleep & Zahnle 2001; Sleep *et al.* 2001).

Ridge outgassing

The oceanic crust is a source of CO_2 when magma upwelling at mid-ocean ridges degasses and later is a sink when circulating sea water reacts with the sea floor at low temperatures. For simplicity, we assume that at first the basalt degasses completely and later, when the basalt is cool, CO_2 is added to it by reaction with sea

water. In reality, some igneous CO_2 is retained by the basalt especially within the dyke complex. Various workers following Alt *et al.* (1986) have reported net gain rather than total CO_2 in their flux estimates.

The degassing flux is proportional to the global rate of crustal production $\partial A/\partial t$, the degassing depth D_s, and the concentration of CO_2 in the mantle:

$$F_{\text{ridge}} = \frac{\partial A}{\partial t} \frac{\rho_s}{\rho_m} \left(\frac{R_{\text{man}}}{V_{\text{man}}} \right) D_s \qquad (9)$$

where ρ_s is the density of the degassed mantle $(3.3\,\text{g cm}^{-3})$, ρ_m is the average mantle density $(4.5\,\text{g cm}^{-3})$, and V_{man} is the volume of the mantle $(8.9 \times 10^{11}\,\text{km}^3)$. The current source depth D_s is well constrained independently of volatiles at about 56 km (Langmuir *et al.* 1992). It is a scale depth for degassing that should not be taken literally as the deepest level where any melt can form. We ignore the undegassed mantle as irrelevant because by definition there is virtually no traffic between it and the surface. If an undegassed mantle were included both R_{man} and V_{man} would be reduced but their ratio unchanged.

The global CO_2 flux is obtained from the $CO_2/$^{3}He ratio in quenched bubbles, quenched glasses or hot hydrothermal fluids, and the known total flux of ^{3}He to the oceans (DesMarais & Moore 1984). Reliable estimates of the ridge flux F_{ridge} are in the range of $(1.5–2.5) \times 10^{12}$ moles a^{-1} (Marty & Jambon 1987; Gerlach 1991; Zhang & Zindler 1993; Goddéris & François 1995; Marty & Tolstikhin 1998). These imply a present mantle reservoir R_{man} between 11×10^{21} and 18×10^{21} moles. Reliable estimates for the flux from plume-derived hotspot magmas are not available. Marty & Tolstikhin (1998) gave an upper limit of 3×10^{12} mole a^{-1} and a negligible lower limit. We do not consider hotspots separately.

Hydrothermal carbonatization

The oceanic crust is a sink for CO_2 by reaction (1). At low temperatures, circulating sea water reacts with the sea floor to form carbonates. Carbonate veins and disseminated carbonate formed in this way have been sampled from the small number of holes that have been drilled deeply into the oceanic crust (Alt & Teagle 1999). The irregular distribution of carbonate within holes and variations between closely spaced holes hinders extrapolation to the global cycle. An indirect approach using geochemistry and heat flow is more practical.

The amount of carbonate added to the oceanic crust can be constrained by chemical analyses of hydrothermal fluids and by using the fluxes of heat and various elements to calibrate the total volume of flow (e.g. François & Walker 1992; Alt 1995; Caldeira 1995; Kadko *et al.* 1995; Stein *et al.* 1995; Brady & Gíslason 1997; Sansone *et al.* 1998). For this purpose, we follow Schultz & Elderfield (1997, 1999) and partition hydrothermal circulation into three regimes: high temperature, *c.* 350°C, axial flow; warm, *c.* 20°C, near-axial flow which extensively reacts with the rock; and cool, *c.* 5°C, off-axial flow through the shallowest ocean crust. The high-temperature flow moves CO_2 from the hot basalt into the ocean. The cold flow circulates through a relatively small volume of shallow crust and is not believed to be significant to the CO_2 cycle. The warm flow appears to be an important CO_2 sink. For example, dissolved CO_2 has been measured from a warm vent on the flank of the Juan de Fuca ridge and found to be 66% depleted relative to normal sea water (Sansone *et al.* 1998).

The flux of warm sea water W through the oceanic crust can be estimated from the measured global sea-floor heat-flow anomaly H and the temperature anomaly T_w of the hydrothermal sea water relative to the bottom of the ocean. H is the difference between the heat flow expected from the cooling oceanic crust (which declines with the square root of age) and the heat flow obtained by directly measuring the temperature gradient and conductivity in the sediments. The difference is ascribed to hydrothermal cooling: H amounts to about 20% of the global oceanic heat flow and occurs mostly in young (<1 Ma) crust, for which the thermal gradient is steep enough that circulating water can reach warm rock. For the flow of water we write

$$W = \frac{H}{T_w C_w \rho_w} \qquad (10)$$

where $\rho_w C_w = 4\,\text{MJ m}^{-3}$ is the heat capacity per unit volume of water. H can be expressed in terms of the rate at which warm new crust is created and the degree to which hydrothermal circulation cools it. New crust is created at the rate $\partial A/\partial t$, currently $3\,\text{km}^2\,\text{a}^{-1}$. The flux of CO_2 into the warm crust is therefore

$$F_{\text{hydro}} = R_{\text{oc}} \left(\frac{W}{V_{\text{oc}}} \right)$$

$$= \frac{H}{\rho_w C_w T_w} \left(\frac{R_{\text{oc}}}{V_{\text{oc}}} \right) \equiv \frac{\partial A}{\partial t} \frac{R_{\text{oc}}}{A_{\text{hydro}}} \qquad (11)$$

in which V_{oc} refers to the volume of the oceans and

$$A_{hydro} \equiv \frac{\partial A}{\partial t} \frac{V_{oc}}{W} \equiv \frac{\partial A}{\partial t} \tau_{hydro}$$

is a constant with units of area; τ_{hydro} is the current time scale for the whole ocean to circulate through these hydrothermal systems.

In practice, W is directly inferred from heat flow and chemical mass balances. Warm hydrothermal flow is a major sink for dissolved oceanic Mg^{2+}. The Mg^{2+} in the warm hydrothermal fluid is removed quantitatively by reaction with basalt. Because the flux of Mg^{2+} into the ocean in river waters and the competing sinks (e.g. clays) can be estimated, the known Mg^{2+} concentration in sea water can be used to determine W. This argument is independent of CO_2.

Using both heat flow and Mg, Schultz & Elderfield (1997, 1999) concluded that 1.5×10^{12} W, or about a quarter of the total global hydrothermal heat flow, escapes through warm vents with an assumed average temperature anomaly of 20 K; the corresponding flux of water is $W = 6.4 \times 10^{11}$ m^3 a^{-1}. The latter implies that the entire ocean circulates through warm vents in $\tau_{hydro} = 2$ Ma, for which $A_{hydro} = 6 \times 10^6$ km^2. In the current ocean a hydrothermal flux equivalent to quantitative extraction of CO_2 on a cycle time of 2 Ma is $F_{hydro} = 1.65 \times 10^{12}$ moles a^{-1}. On the other hand, using similar data, Sansone *et al.* (1998) argue for warmer vents (temperature anomaly 64 K) that carry a somewhat smaller fraction (8–20%) of the global hydrothermal heat flow. Their estimates translate into smaller amounts of water circulating over longer time scales, $8 < \tau_{hydro} < 20$ Ma, for which $2.4 \times 10^7 < A_{hydro} < 6 \times 10^7$ km^2. For comparison, Walker (1985) uses 10 Ma for this cycle. As the actual flux is uncertain, we use Schultz & Elderfield's (1997, 1999) estimate as a lower limit on A_{hydro}. We use the higher of Sansone *et al.*'s (1998) estimates as our upper limit.

An illustrative example

The simplest case is to consider the steady-state value of the oceanic–atmospheric carbon dioxide reservoir R_{oc} that results from equating mantle outgassing to ingassing by subduction. From equation (7), the condition for steady state is $F_{ridge} = C_{deep}F_{hydro}$. Using equation (9) for F_{ridge} and equation (11) for F_{hydro}, we obtain a steady-state reservoir size of

$$\langle R_{oc} \rangle = \frac{A_{hydro}D_s}{V_{man}C_{deep}} \frac{\rho_s}{\rho_m} R_{man}. \qquad (12)$$

This expression is independent of the rate of crustal overturn: to first approximation the amount of CO_2 in the ocean and atmosphere does not depend on global heat flow. If we set the constant $A_{hydro} = 1 \times 10^7$ km^2, take $11\times 10^{21} < R_{man} < 18 \times 10^{21}$ moles, take $D_s = 56$ km, and $C_{deep} = 0.75$, the current steady-state value of R_{oc} would be $(6.6-11) \times 10^{18}$ moles. This is comparable with the current amount of 3.3×10^{18} moles. Assuming the same partitioning between ocean and atmosphere as today, this steady-state value of R_{oc} is equivalent to $2.0 < pCO_2 < 3.4$ PAL, an amount not differing significantly from what it has been on average over the past hundred million years or so. What is most interesting about this near coincidence is that (1) it is obtained based on geological and geochemical arguments in which CO_2 plays no part and (2) it ignores the continents and the Urey cycle. With A_{hydro} fixed, D_s doubled and C_{deep} halved, equation (12) predicts an Archaean CO_2 level of just 8–14 PAL.

Hydrothermal carbonatization, redux

To extrapolate the sea-floor weathering flux F_{hydro} into the past requires a model of the water–rock reaction. There are two important possibilities, depending on whether the reactable cations are more or less abundant than CO_2. In equation (11) we implicitly assume that CO_2 is quantitatively removed from the sea water. In effect we presume fast reactions with superabundant cations. Walker (1985) and François & Walker (1992) assumed that CO_2 is removed in linear proportion to its concentration. This differs from our picture only in the value of A_{hydro}: in either model it is the delivery of CO_2-rich waters to the oceanic crust by hydrothermal circulation that limits uptake, so that CO_2 is quantitatively depleted in the circulating sea water until available CaO, MgO and FeO in the rock are exhausted.

However, there is some experimental evidence that this reaction is not strongly dependent on CO_2 or pH (Caldeira 1995; Brady & Gíslason 1997). In these experiments reaction rates are kinetically limited by the availability of cations. If this is the case in real hydrothermal systems, then it is possible that the uptake of CO_2 by the sea floor has always been similar to what it is at present, as Caldeira (1995), Goddéris & François (1995) and Brady & Gíslason (1997) assumed. This would make the current rough equality between subduction and ridge degassing rates in equation (12) a coincidence, and leave as an open puzzle how the mantle CO_2 cycle is to be closed over long time scales.

In view of these uncertainties, we will write $F_{hydro} \propto pCO_2^{\alpha}$, where the parameter α represents the dependence of hydrothermal carbonatization on pCO_2. Quantitative depletion corresponds to $\alpha = 1$. Sansone et al's data imply something short of this. Brady & Gíslason's laboratory data correspond to $\alpha = 0.23$, but of course their data are for reactions running enormously faster than in nature. We can test these different assumptions at a higher CO_2 concentration by comparing reconstructed CO_2 levels with the observed carbonate in Mesozoic ocean cores. As noted, quantitative extraction of CO_2 in the current ocean over $\tau_{hydro} = 2$ Ma corresponds to $F_{hydro} \times 1.65 \times 10^{12}$ moles a^{-1}. This flux is compatible with what is known about the abundance of carbonate from holes drilled into layer 2A of the oceanic crust. Using $\alpha = 1$ and $F_{sub} = 3.4 \times 10^{12}$ mole a^{-1} (the current rate at which carbonatized sea floor is entering subduction zones; see above) implies that the Mesozoic oceans contained about 7×10^{18} moles of CO_2. This is comparable with Lasaga et al.'s (1985) estimate of 10×10^{18} moles of CO_2 (i.e. 3 PAL). On the other hand, Ekart et al.'s (1999) more direct estimate from palaeosol data that pCO_2 was as high as 8 PAL in the Mesozoic is consistent with $\alpha \approx 0.4$.

It is possible that some of the carbonate lost from the circulating hydrothermal fluid has simply precipitated because the sea water has been heated (M. Bickel, pers. comm.). If so, then both the carbonate and the cation are supplied by the sea water. If the ultimate source of the cations is continental weathering, the precipitated carbonate would be equivalent to a pelagic carbonate and not true sea-floor weathering; whereas if the ultimate source of the cation is somewhere else in the sea floor, then for accounting purposes precipitation is equivalent to in situ reaction. Solubility of $CaCO_3$ is not a strong enough function of temperature for temperature alone to cause quantitative precipitation of sea water calcium carbonate. The effect of pH is probably greater, but such fluids develop high pH by reaction with the rock. Currently the Ca/bicarbonate ratio in sea water is about four. If the Ca that precipitated had been extracted from the sea floor (as we surmise) this would amount to but one part in five of the calcium. As we go back in time saturation of $CaCO_3$ requires higher levels of pCO_2 that imply lower levels of Ca in seawater. A value of 4 PAL CO_2 reverses the ratio of Ca to bicarbonate. Thus in Mesozoic time (taking $pCO_2 = 4$ PAL for the illustration), quantitative carbonatization of sea floor basalts would have required that 3/4 of the calcium be scavenged from the basalt itself. As discussed above, the Mesozoic sea floor appears to have been well carbonatized. Sea-floor weathering as we have described it is implicated.

Oceanic pH

Oceanic pH controls the partitioning of CO_2 between the ocean and the atmosphere and hence controls pCO_2 given R_{oc}. Over geological times, the pH of the modern ocean is dynamically buffered by low-temperature weathering and sea-floor alteration of silicates (which produce alkaline waters) and high-temperature axial hydrothermal circulation (which produces acid waters) (e.g. Grotzinger & Kasting 1993). The relative importance of high-temperature and low-temperature vents on the early Earth is debated. Kempe & Kazmierczak (1994) noted that impact ejecta and vigorous tectonic activity on the early Earth would have exposed much more rock to low-temperature alteration, and that fluids reacting with Archaean komatiitic lavas are more alkaline than those reacting with modern basalts. They contended that the early ocean was significantly more alkaline than the present ocean. Macloed et al. (1994) and Russell & Hall (1997) in contrast focused on the large amount of hot hydrothermal activity on the early Earth and contended that the early ocean was acid and that low-temperature hydrothermal vents served only to produce local alkaline conditions. Direct evidence to support either position is at best model dependent. We have no strong reason to expect the relative proportions of high- and low-temperature hydrothermal systems to differ between Archaean time and today. In particular, the bulk of both the low- and high-temperature alteration occurs within young crust near the ridge axis, implying that the lifetime of oceanic crust is not a major factor. It is a reasonable compromise for the present to regard pH as fixed in our calculations. We note that the CO_2 levels we predict for the atmosphere depend strongly on pH. A more alkaline ocean, which we expect for Hadean time when impact ejecta are important, would remove more CO_2 from the atmosphere.

Ancient CO_2 cycles

Extrapolating the CO_2 cycle into ancient times requires us first to consider what happens when plate tectonic cycles run more quickly and then, for earlier times, to consider effects that are no longer important on Earth. In order of increasing ancestry and uncertainty, we consider higher heat flows and related issues within the constraints of plate tectonics, and then abundant

impact ejecta as a major source of easily weath-ered and subductable mafic materials.

Archaean cycle

We solve the time-dependent problem with the coupled equations (4)–(6) using R_{oc}, T and pCO_2 obtained solving equations (7) and (8) in steady state. As above, we let the heat flow evolve as $Q(t) = (1 - t/4.5)^{\mu}$, with $\mu = 0.7$ or $\mu = 0.2$ for high or low heat flow, respectively. The metamorphic flux F_{meta} is assumed propor-tional to the product of the heat flow and the continental carbonate reservoir, QR_{con}. We use equation (9) for the mid-ocean degassing flux F_{ridge} and equation (11) for the sea-floor weath-ering flux F_{hydro}. In our standard models we take the degassing depth to decrease as the mantle cools. We write this as $D_s = 56 \, \text{km} \, (1 + t/3 \, \text{Ga})$ for $t < 3 \, \text{Ga}$ and $D_s = 112 \, \text{km}$ for $t > 3 \, \text{Ga}$. We also assume that subduction of carbonate to the mantle is less efficient when the mantle is hotter than today. We assume C_{deep} is inversely pro-portional to D_s. We take the sea-floor creation rate to go as the heat flow squared, $\partial A/\partial t \propto Q^2$, the relationship predicted by plate tectonics. For comparison we also consider what would happen if plate tectonics enforces a more con-stant heat flow (see below). In these models we hold Q constant, but D_s and C_{deep}, because they depend on mantle temperature, both evolve as in the standard case. In all cases we take $F_{hydro} \propto R_{oc}^{\alpha}$. Adopted parameters are shown in Figure 3.

We calibrate all models to give the current crustal reservoir R_{con} and an average pCO_2 over the past 400 Ma of 3 PAL. For any model we can do this by adjusting two of four parameters. The four are the hydrothermal circulation constant A_{hydro}; the dependence of sea-floor uptake on pCO_2 represented by α; the calibra-tion of the silicate weathering rate C_{SiO_3w}; and the size of the mantle reservoir R_{man}. The last of these is directly proportional to the mid-ocean ridge outgassing flux F_{ridge}. The mantle degas-sing time and degassing depth D_s are not free
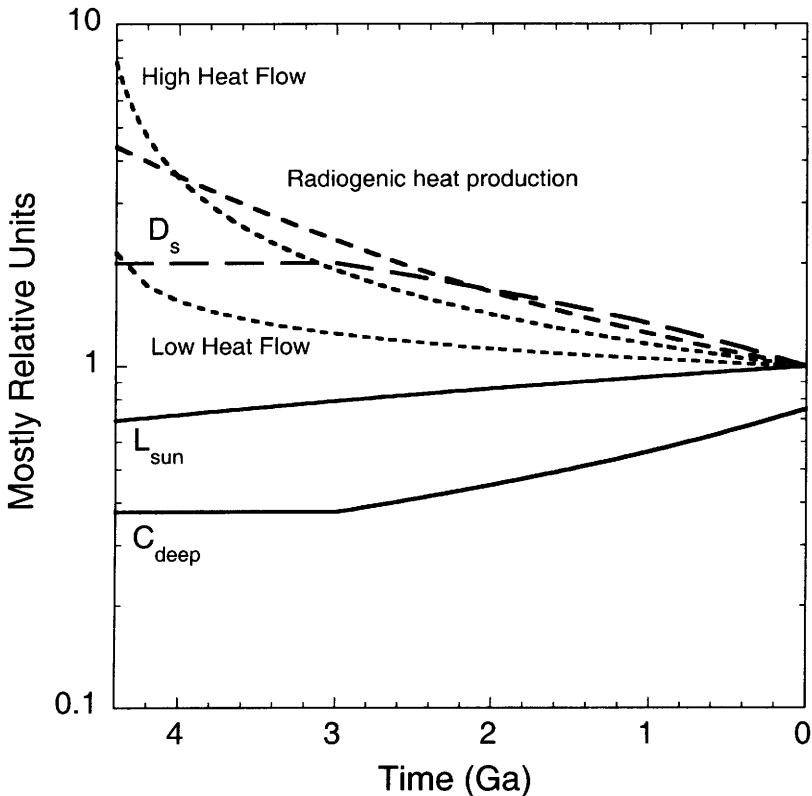

Fig. 3. Relative values of some model parameters through Earth history. Both high and low heat-flow histories are indicated; these are compared with the history of radiogenic heating.

parameters because they are constrained independently of CO_2. Of the four, A_{hydro} and F_{ridge} are observables subject to constraints discussed above. The power α may be near unity but for our purposes it is best regarded as free, as together with A_{hydro} it determines the return flux to the mantle.

Standard models. Figure 4 shows loci of successful standard models as functions of the observables A_{hydro} and F_{ridge}, the warm hydrothermal circulation constant and the mid-ocean ridge outgassing flux, respectively. Heat flow is high ($\mu = 0.7$). The models assume a current continental inventory $F_{con} = 5 \times 10^{21}$ moles. Curves

are labelled by α. The fourth parameter, C_{SiO_3w} (not shown), tunes the Urey cycle and needs to be set separately for each model. In successful models F_{SiO_3w} is typically about 10–20% smaller than F_{meta}. Initial conditions are unimportant. Indicated in the figure are two particular models with $F_{ridge} = 2 \times 10^{12}$ moles a^{-1} and different values of A_{hydro} and α. Surface temperature and pCO_2 histories for these models are shown in Figure 5. These compare different dependences of sea-floor weathering on pCO_2 (i.e. different values of α). Lower values of α require faster hydrothermal cycling.

The finite volume of reactable basaltic crust is not explicitly accounted for in these models.
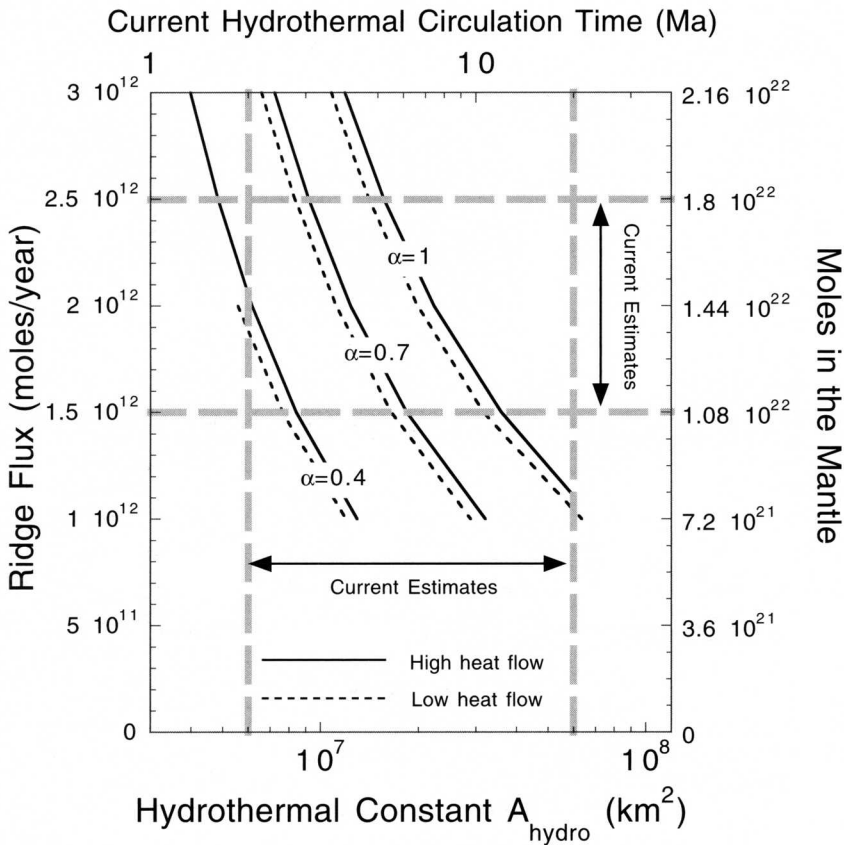

Fig. 4. Parameter choices that cause our model of coupled continental and mantle CO_2 cycles to converge to modern atmospheric and continental CO_2 inventories. We presume standard solar evolution and CO_2 working alone as the greenhouse gas. Quantitative values for the hydrothermal circulation time scale τ_{hydro} and the mid-ocean ridge degassing flux F_{ridge} refer to present values. The mantle inventory presumes whole-mantle convection. The hydrothermal circulation constant A_{hydro} is related to τ_{hydro} and the crustal creation rate $\partial A/\partial t$ by $A_{hydro} = \partial A/\partial t \times \tau_{hydro}$. Best estimates of A_{hydro} and F_{ridge} are discussed in the text. The parameter α represents the dependence of sea-floor carbonatization on the concentration of CO_2 in sea water. The different heat-flow histories are labelled 'high' and 'low' according to heat flow in Archaean time; the low heat-flow models have heat flow that changes relatively little over the past 4 Ga.
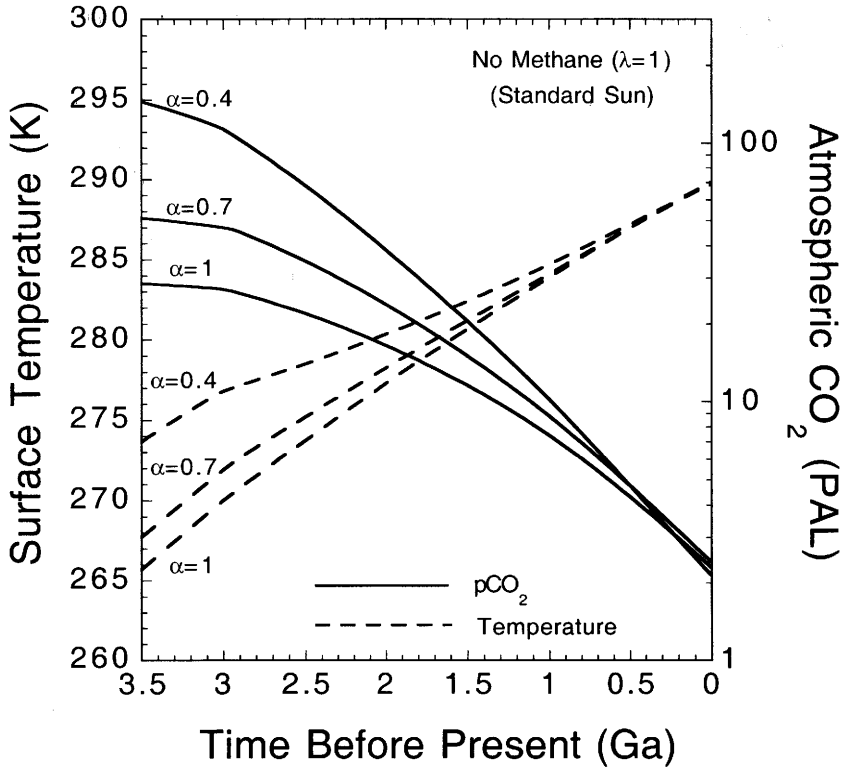
Fig. 5. Global surface temperature and pCO_2 histories for three high heat flow models with different values of α, the CO_2 dependence of the sea-floor weathering rate. The models assume a current mid-ocean ridge flux $F_{ridge} = 2 \times 10^{12}$ moles a^{-1}. Models with higher values of α require higher amounts of CO_2 to obtain the same amount of CO_2 consumption.

A half-kilometre of basalt, a thickness comparable with the modern permeable and reactable layer 2A at fast ridges (it is somewhat thicker at slow ridges, e.g. Hooft *et al.* (1996)), if fully carbonatized, would yield 300 m of carbonate, or $R_{bas} = 3 \times 10^{12}$ moles. This limit is approached but not exceeded in any of the models discussed here. Our upper limit on the current inventory of carbonatized basalt is equivalent to 40 m of carbonate (i.e. *c.* 10% carbonatization). A value of α near unity is not unreasonable for carbonatization levels <10% but is untenable if carbonatization levels become much higher. Doubtless the carbonatized layer deepens as CO_2 levels increase, but this requires reaction of increasingly impermeable media, with $\alpha \ll 1$. A related issue is that, in our models, the capacity of the basalt to hold carbonate is exceeded if $C_{deep} < 0.2$ In such conditions CO_2 can build up hugely in the atmosphere, oceans, and on the sea floor, and the surface might become very hot indeed. We have considered such cases in more detail elsewhere (Sleep & Zahnle 2001; Sleep *et al.* 2001).

Lower heat flow. Our standard higher heat flow assumption is that heat flow Q declined over time somewhat more slowly than radioactive heat generation declined. Although this seems a reasonable assumption it is not especially well supported. In particular, argon degassing of the Earth is consistent with no change in sea-floor spreading rate over 3 Ga (Sleep 1979; Tajika & Matsui 1993). Some theories also suggest that plate tectonics should occur at a relatively constant rate as the mantle cools (F. Nimmo, pers. comm.). Constant heat flow implies that only about half the mantle has cycled through the mid-ocean ridges over the past 3.5 Ga; this slow circulation maintains large geochemically isolated reservoirs without appealing to layered convection. To test the influence of low heat flow we use $Q(t) = (1 - t/4.5)^\mu$ with $\mu = 0.2$ as a lower bound. This parameterization predicts heat flow today that is twice the current rate of radiogenic heating, but *c.* 3.5 Ga the heat flow is some 10% less than radiogenic heating. The more nearly constant heat flow implies that the

hydrothermal sink, subduction, and even continental metamorphism are also nearly constant. Because the mantle has cooled 150–200 K since Archaean time (Abbott *et al.* 1994), processes that depend directly on the temperature of the mantle (the partial melting depth D_s and the subduction efficiency C_{deep}) evolve as in the standard model.

Figure 4 shows loci of successful constant heat-flow models as functions of the observables A_{hydro} and F_{ridge}. Overall the low and high heat-flow models have similar requirements. Figure 6 which compares two specific models with $\alpha = 0.7$, shows that heat flow has relatively little effect on either temperature or pCO_2. This insensitivity to heat flow was anticipated by the steady-state estimate, equation (12) above, in which the crustal creation rate plays no part. In detail, the low heat-flow models are slightly cooler, owing to a smaller metamorphic source of CO_2. In turn, the smaller value of pCO_2 requires somewhat higher amounts of hydrothermal circulation to maintain the return cycle

to the mantle. We will find below that heat flow is important in Hadean time, where impact ejecta compete with new oceanic crust for CO_2.

Effect of another greenhouse gas. The standard models violate the constraint on pCO_2 inferred from palaeosols dated *c.* 2.75 Ga (Rye *et al.* 1995). This confrontation with the datum is the subject of Figure 7. Rye *et al.* showed that Caldeira & Kasting's (1992) climate parameterization for 2.75 Ga implies that siderite would have been stable in soils unless temperatures were below freezing. Iron was present in these soils but siderite was not. There are three ways to resolve this paradox. (1) The palaeosol may represent a local region or time when the temperature was higher than the global average. For example, Ekart *et al.* (1999) argued that palaeosols record the warmest times of the year, with a typical overestimate of about 10°C for a temperate climate. We therefore also show Rye *et al.*'s curve offset by 10°C. Doing so eliminates
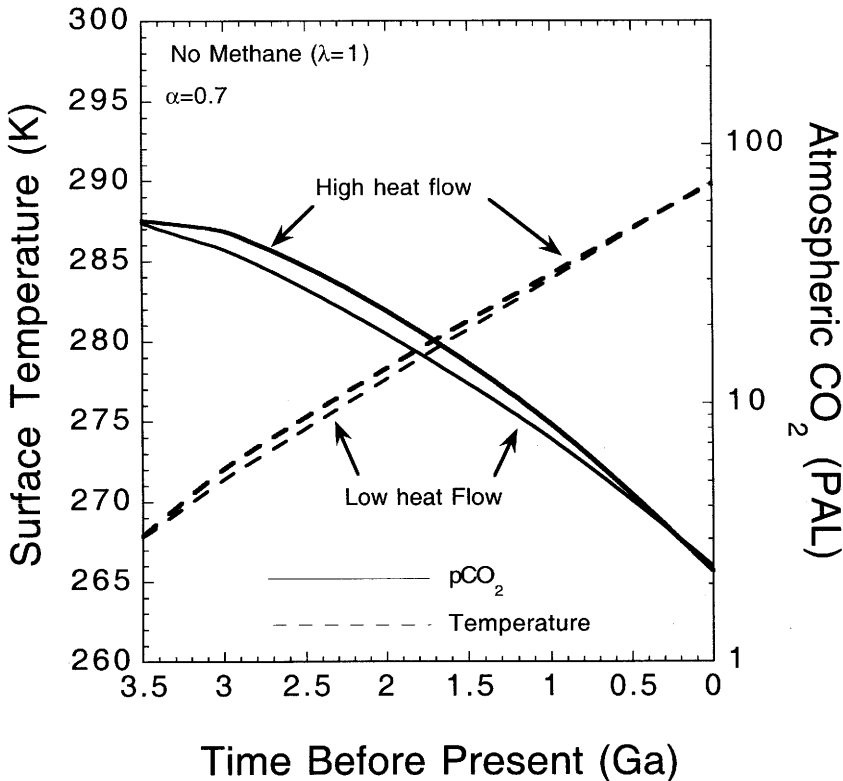

Fig. 6. Global surface temperature and pCO_2 histories for two otherwise identical models with high and low heat flows. The models assume a current mid-ocean ridge flux $F_{ridge} = 2 \times 10^{12}$ moles a^{-1}. The low heat-flow models feature relatively little secular change in the oceanic crustal creation rate and the continental metamorphic recycling rate.
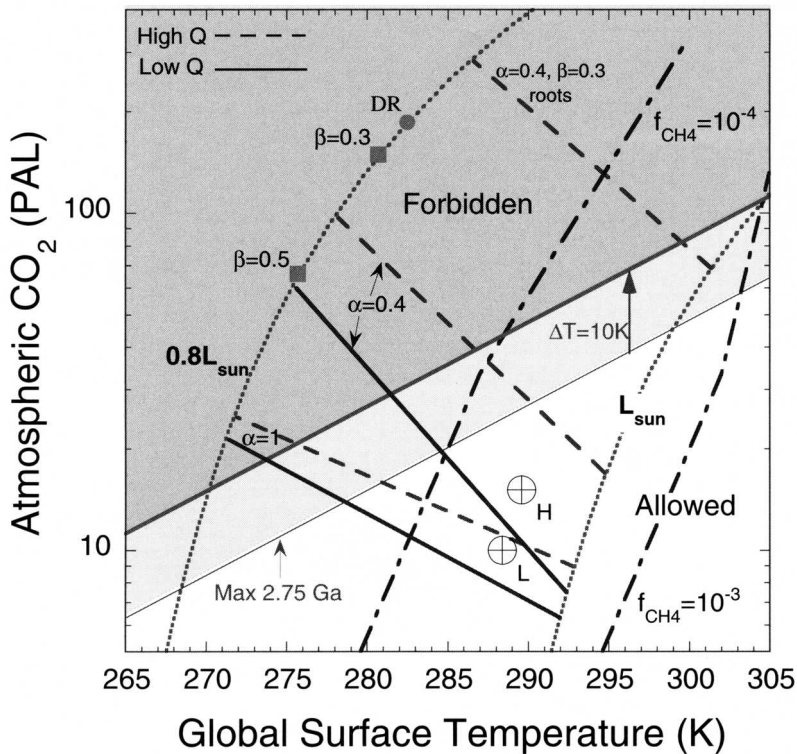
Fig. 7. The figure shows the relationship between pCO_2 and global average surface temperature for 2.75 Ga, and compares this with the siderite stability field (lightly shaded region) deduced by Rye *et al.* (1995). Siderite is a constraint because it was absent in a 2.75 Ga palaeosol (Rye *et al.* 1995). The expected seasonal bias in weathering rates (Ekart *et al.* 1999) relaxes the constraint by some 10 K; the relaxed constraint is indicated by darker shading. The curve labelled $L = 0.8L_{sun}$ shows CO_2's greenhouse effect for nominal insolation (Caldeira & Kasting 1992). Where the models in Figures 1 and 2 plot on this curve is indicated ('DR' denotes 'Devonian roots'). No model on the $L = 0.8L_{sun}$ curve is compatible with the siderite constraint. Either the palaeosol represents a special locality or other greenhouse gases were present. To illustrate the latter, we show CO_2 greenhouses consistent with current insolation ($L = L_{sun}$) and two methane–CO_2 greenhouses consistent with $L = 0.8L_{sun}$ (Pavlov *et al.* 2000). The latter are labelled by methane mixing ratio. Because the $L = L_{sun}$ and the $f_{CH_4} = 10^{-4}$ curves are nearly parallel, we can vary the effective solar luminosity as a proxy for different greenhouses. The five nearly straight lines connecting the $L = L_{sun}$ and the $L = 0.8L_{sun}$ curves show our model predictions for the climate at 2.75 Ga, treating different amounts of methane by varying $0 < \lambda < 1$ in equation (13). Predicted climates are nearly independent of the mid-ocean ridge degassing flux F_{ridge}. Continuous lines are for high Archaean heat flow; broken lines for low Archaean heat flow. These models are addressed by Figures 4–6 and 8 and 9. The different values of α are meant to span the plausible range of sea-floor weathering rates. The high Q model labelled '$\alpha = 0.4 +$ roots' uses a slower weathering rate before the appearance of land plants with root systems. It maximizes pCO_2 within the context of our models. This model and others like it are addressed by Figures 10 and 11. Finally, the two models labelled '$\oplus$' use $\alpha = 0.7$ and $\lambda = 0.2$ (equivalent to *c*. 250 ppm CH_4) and the two different heat flow histories. These models are singled out to illustrate the evolution of reservoirs and fluxes in Figures 12–15.

some of the perceived discrepancy. (2) Rye *et al.* (1995) have the siderite stability field wrong. (3) Other greenhouse gases may have been present, methane in particular.

Here we pursue the more interesting possibility: another greenhouse gas, methane, was impor-

tant (Kiehl & Dickinson, 1987; Pavlov *et al.* 2000). Biologically generated methane is expected to have been present in the atmosphere at levels of hundreds of ppm before the rise of oxygen. Even after oxygen rose to levels of order 0.1 PAL, methane was plausibly present at tens of ppm.

We use the convenient method of modifying the solar luminosity as a proxy for the increased greenhouse effect. We use the arbitrary function

$$L = L_0(1 - 0.07\lambda t) \qquad (13)$$

with $\lambda = 0.2$ rather than the standard $\lambda = 1$. This is equivalent to some 250 ppm CH_4 c. 2.75 Ga (see Fig. 7). We will call these 'high methane' rather than 'bright Sun' models, to focus attention on a physically plausible explanation for the temperate climate of ancient Earth. The calculations are performed for all of Earth history even though high levels of methane are inconsistent with the modern atmosphere.

Loci of permitted high methane models are plotted in Figure 8. It should be noted that these models require much higher rates of hydrothermal circulation (lower values of A_{hydro}) than do the standard Sun models. This is required for sea-floor weathering to compete with continental weathering, the rates of which are higher because of the higher surface temperature (recall that sea-floor weathering closes the mantle's CO_2 cycle in our models). Computed temperature and carbon dioxide histories for $\alpha = 0.7$ and different levels of methane are compared with the standard model (also with $\alpha = 0.7$) in Figure 9. As expected, the warmer climates result in less atmospheric CO_2.

Figure 7 compares predictions for 2.75 Ga by two families of models to the local temperature and pCO_2 limits obtained by Rye et al. (1995). The region below the siderite stability field is
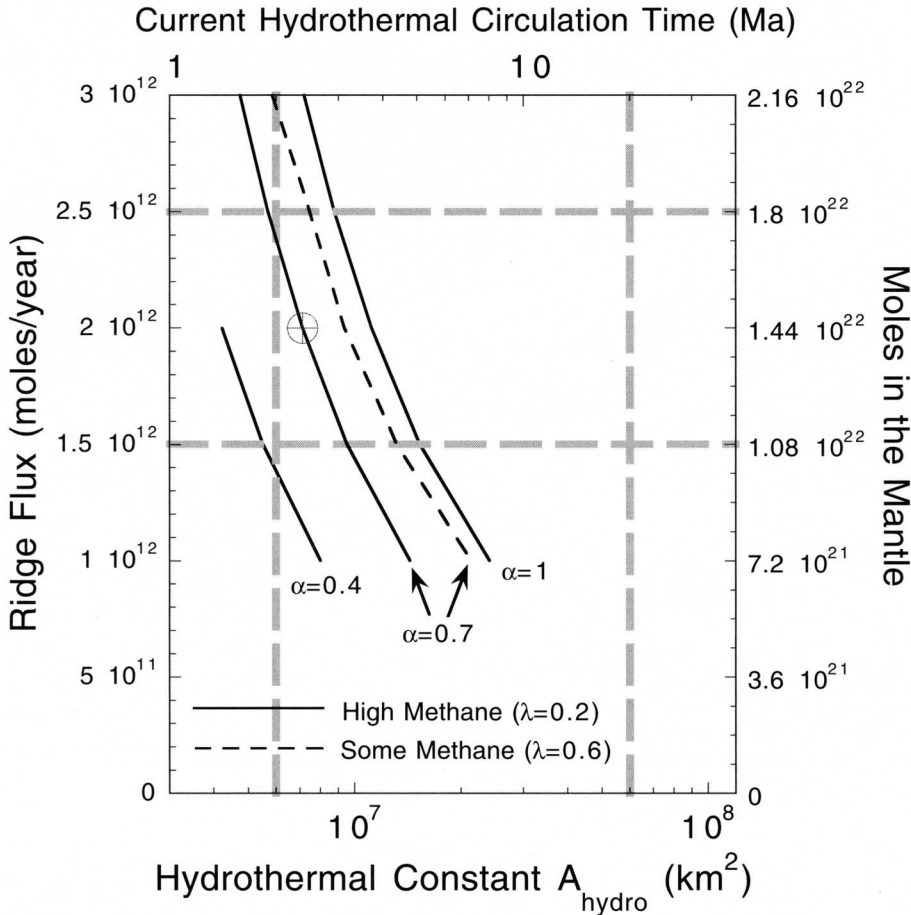

Fig. 8. Parameter choices that converge to modern atmospheric and continental CO_2 inventories for models with methane as an additional greenhouse gas. These models imply relatively low levels of CO_2, which in turn requires that hydrothermal circulation be relatively more efficient if it is to return CO_2 to the mantle. The specific model indicated by the '⊕' symbol is discussed in more detail in Figures 7 and 12–15.

forbidden. We generate surface temperatures and pCO_2 by letting λ range from one to zero. Each model is constrained to evolve to $R_{con} = 5 \times 10^{21}$ moles and an average value of $pCO_2 = 3$ PAL over the past 400 Ma. The standard faint Sun ($\lambda = 1$) and the nonstandard bright Sun ($\lambda = 0.2$) are shown. Shown for comparison are loci of pCO_2 and T consistent with different amounts of methane (Pavlov *et al.* 2000). It should be noted that curves of constant methane parallel the curves with $\lambda = 1$ and $\lambda = 0.2$, thus justifying somewhat λ as a proxy for methane as a greenhouse gas. We indicate a particular pair of models (the '$\oplus$' symbols in Fig. 7) with $\alpha = 0.7$ and $\lambda = 0.2$ (corresponding to $c. 250\,ppm$ CH_4), but different heat-flow histories, to discuss in more detail below.

Effect of land plants. Land plants with roots have existed only since Devonian time (e.g. Berner, 1997). It might be expected that chemical weathering was sluggish before then (Berner 1997). We use this possibility to illustrate the general conclusion that a clement climate, CO_2 rich, could have existed in Archaean time if both silicate weathering and carbonitization of oceanic crust were sluggish sinks requiring high pCO_2 to operate. It should be noted that these models are mirror images of the high methane models, in that they address the faint early Sun by invoking biological measures to raise CO_2.

To quantify the effect of roots, we compute models based on the situation envisioned by Berner (1997). Our 'roots' models differ from the rootless models by setting the weathering rate
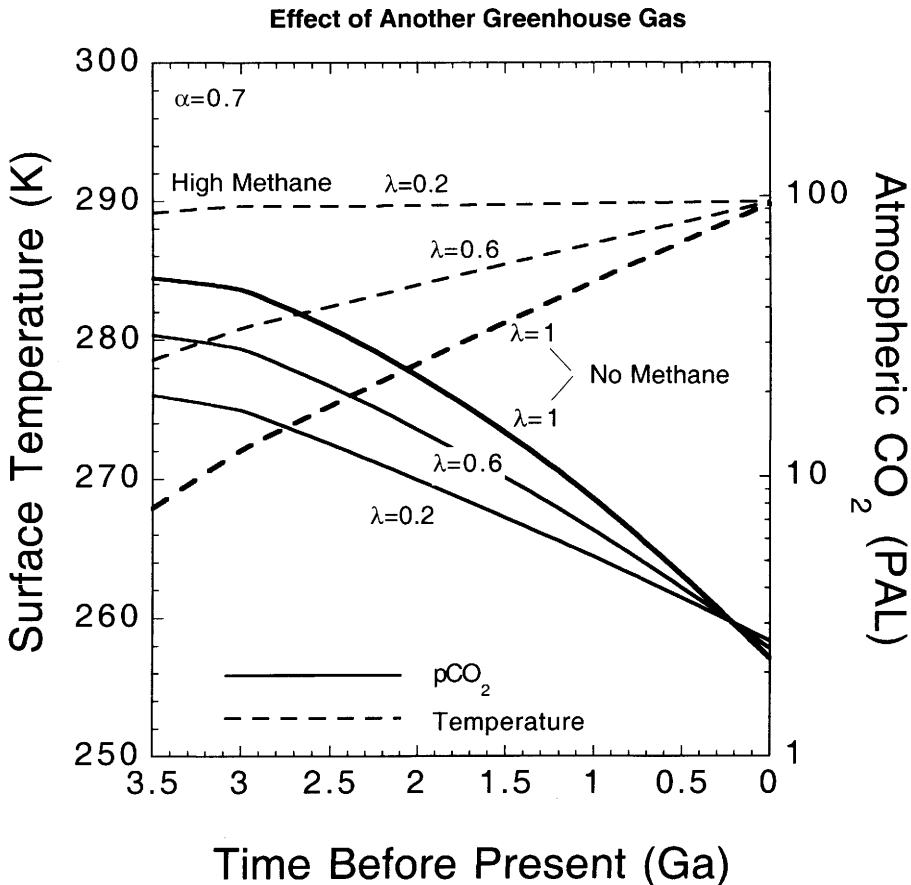

Fig. 9. Global surface temperature and pCO_2 histories for models with different amounts of methane. The models assume a current mid-ocean ridge flux $F_{ridge} = 2 \times 10^{12}$ moles a^{-1}. The 'methane' models are constructed by arbitrarily reducing the rate of solar luminosity evolution by the factor λ in equation (13). The added greenhouse effect of the methane produces warmer climates that speed silicate weathering, significantly reducing pCO_2 and thereby indicating that silicate weathering has a significant effect throughout Earth history.

before the advent of roots to 33% of the current rate, and for better consistency with Berner (1994) we consider cases with $\beta = 0.5$ as well as $\beta = 0.3$. Figure 10, the rooted analogue to Figures 4 and 8 shows what parameter values will evolve to modern conditions. Two models with $\alpha = 0.5$ and $F_{ridge} = 2 \times 10^{12}$ moles a^{-1} but different β are paid more attention in Figure 11. Sluggish weathering before the Devonian period results in higher surface temperatures (Fig. 11) and higher pCO_2, as expected. Efficacy of sea-floor carbonatization must then be smaller. With $\alpha = 0.4$ the oceanic sink is smaller and temperate conditions exist throughout Archaean and

Proterozoic time, with the warmest climates characterizing early Phanerozoic time.

'Roots' models for $\alpha = 0.4$, $\beta = 0.3$ and different suns ($0 < \lambda < 1$) are compared with Rye et al.'s palaeosol constraint in Figure 7. Rooted models for $\alpha = 1$ (not shown) roughly coincide with $\alpha = 0.4$ rootless models. By construction the rooted models predict higher pCO_2 levels and warmer Earths than do the rootless models. This makes the rooted models harder to reconcile with Rye et al.'s constraint. On the other hand the rooted models are better suited to keeping Earth warm after the rise of oxygen, when a methane greenhouse is less plausible.
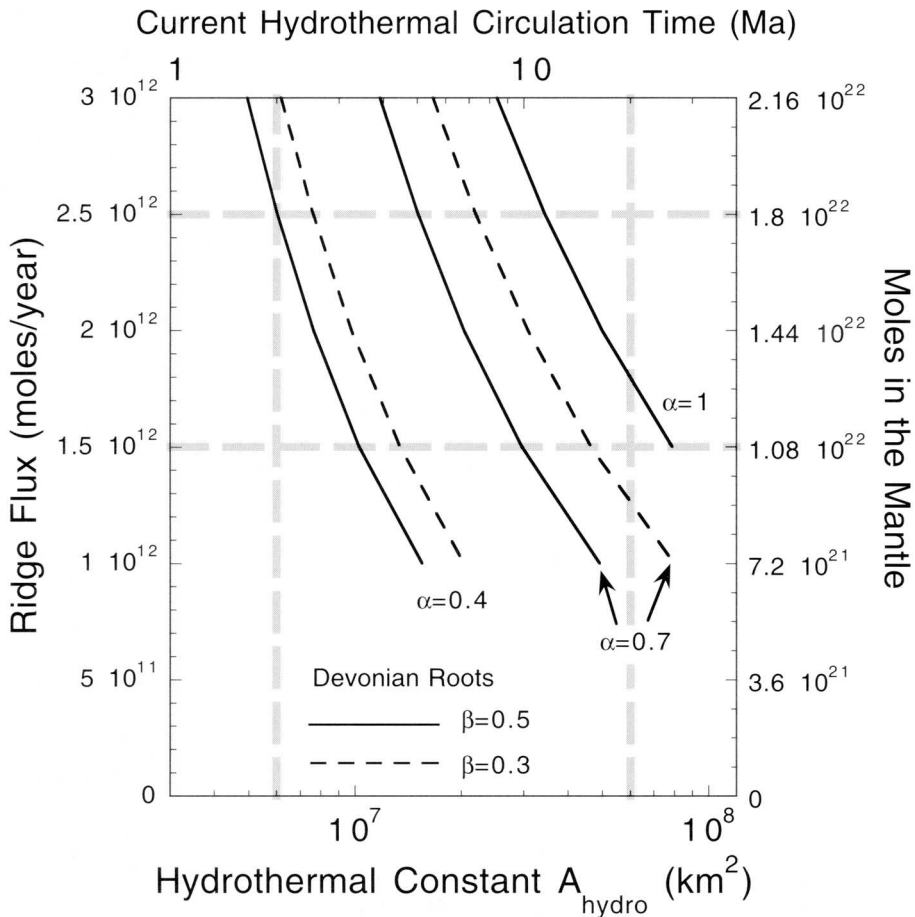

Fig. 10. Parameter choices that converge to modern atmospheric and continental CO_2 inventories for models in which weathering rates increase abruptly upon the advent of roots. These use either $\beta = 0.3$ or $\beta = 0.5$ in equation (8), and reduce the silicate weathering constant (in equation (8)) before the advent of roots to 33% of what it is now. These values are consistent with Berner (1994, 1997)]. These models imply that the ancient atmosphere was fairly CO_2 rich, and so sea-floor weathering needs to have been relatively inefficient or too much CO_2 would have been captured by the mantle.
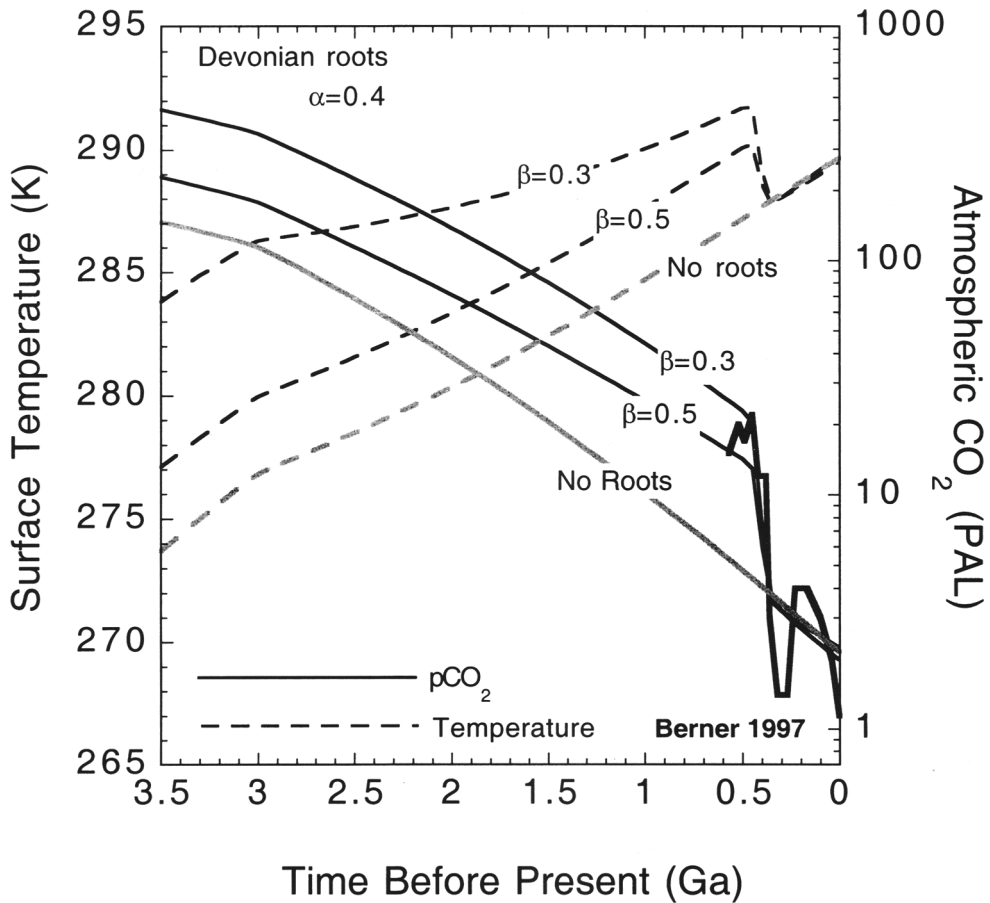
Fig. 11. Surface temperature and pCO_2 histories for some rooted models with current $F_{ridge} = 2 \times 10^{12}$ moles a^{-1}. These are compared with the the standard rootless model (Fig. 6). Also shown for comparison is Berner's (1997) Phanerozoic pCO_2 curve. By choosing favourable parameters ($\alpha = 0.4$, $\beta = 0.3$) we are able to construct a model that maintains a clement Earth using CO_2 alone through most of Earth history. However, such a model badly violates Rye *et al.*'s constraint on pCO_2 (Fig. 7). It is also worth asking whether such models can be consistent with cold climates at the end of Precambrian time.

The Hadean cycle and impact ejecta

The Hadean eon brought an additional threat to CO_2. During Hadean time, impact ejecta would have been quantitatively important sediments (Koster van Groos 1987). Qualitatively, impact ejecta differ from most other sediments in being pulverized, vitrified or otherwise mechanically damaged, and so relatively easily chemically attacked. Ejecta also tended to be more mafic than conventional sediments, because the most frequent target was oceanic basalt and large impacts excavated material from the mantle. Like other oceanic sediments, weathered ejecta would have been subducted along with the plates on which they accumulated. With more buffer-

ing by basic and ultrabasic rocks, and with most of the weathering occurring at relatively low temperatures, the sink for CO_2 would have been greater and the pH may have been higher (Kempe & Degens 1985; Kempe & Kazmierczak 1994). Here we summarize how we parameterized ejecta weathering in our earlier study (Sleep & Zahnle 2001), and in the process correct some errors that marred our first iteration.

The Hadean impact record is best calibrated to the large lunar basins (Zahnle & Sleep 1996; Anbar *et al.* 2001). To order of magnitude, the mass of the typical basin-forming impactor was *c.* 10^{20} g although the archtypes (e.g. Orientale) were larger, *c.* 10^{21} g and the largest that remains clearly visible (S. Pole–Aitken), perhaps

$c.\,10^{22}$ g. The last of the lunar basins formed $c.\,3.8$–3.85 Ga, so that to first approximation the average lunar impact rate during Hadean time as a whole (6×10^8 a) was $> 5 \times 10^{13}$ g a^{-1}. At 3.85 Ga the average impact rate was still very high, $> 10^{13}$ g a^{-1}, and possibly as high as 10^{14} g a^{-1}. Taking into account gravitational focusing and Earth's much larger cross-section, these lunar accretion rates correspond to average Hadean terrestrial accretion rates of 10^{15}–10^{16} g a^{-1}. We will be conservative and use 10^{15} g a^{-1} for 3.8–3.9 Ga. The median value is lower and depends on the time scale over which the impacts are sampled. On the time scale of Earth's resurfacing, the median value of the terrestrial accretion rate at 3.85 Ga would have been $c.\,2 \times 10^{14}$ g a^{-1}. The dependence of the observed accretion rate on the sampling time scale has been discussed in detail by Anbar *et al.* (2001).

To estimate the mass of reactable ejecta we begin with the total mass of ejecta, as defined by the volume of the crater. According to Schmidt & Housen (1987)

$$m_{ej} = 0.13 m_i (\rho_t/m_i)^{0.217} g^{-0.65} v_i^{1.3} \qquad (14)$$

where m_i is the impactor's mass, ρ_t the target density, g gravity, and v_i the impactor's velocity. For $v_i = 15$ km s^{-1} and $\rho_t = 2.86$ g cm^{-3}, the ejected mass is

$$m_{ej} = 2.5 \times 10^{19} (m_i/10^{18})^{0.783} \text{ g} \qquad (15)$$

where the impactor mass is also in grams. For a 10^{21} g impactor, $m_{ej} \approx 5.6 m_i$. If we assume a plausible power-law mass distribution for the impactors,

$$N(>m) \approx (m/m_{max})^{-b} \qquad (16)$$

where $N(>m)$ is the cumulative number of objects greater than mass m, m_{max} is the mass of the largest object in the distribution and $b \approx 0.8$, the ejecta accumulation rate is

$$\dot{M}_{ej} = \int \left(-\frac{\partial \dot{N}}{\partial m} \right) m_{ej}(m)\, dm$$

$$\approx b \frac{m_{max}^b}{\tau_{Had}} \int m_{ej}(m) m^{-1-b}\, dm. \qquad (17)$$

The integral in equation (17) takes an especially simple form for $b = 0.783$:

$$\dot{M}_{ej} \approx \left(\frac{m_{max}}{10^{18}} \right)^{0.783} \frac{2 \times 10^{19}}{\tau_{Had}} \ln \left(\frac{m_{max}}{m_{min}} \right)$$

$$\approx 1 \times 10^{16} \text{ g a}^{-1} \qquad (18)$$

evaluated for $m_{min} = 10^{16}$ g and $m_{max} = 10^{23}$ g. For an ocean-covered Earth, m_{min} is equivalent

to the smallest impactor that can both penetrate the ocean and excavate pristine basalt. The mass of the largest impact is estimated from the total mass accreted, using the rough approximation $m_{max} \approx (1 - b)M_{tot}/b$. We take $\tau_{Had} = 300$ Ma for late Hadean time. The logarithmic dependence makes equation (18) insensitive to specific choices of m_{max} and m_{min}. The logarithmic dependence also indicates that, unlike the iridium accumulation rate (which tracks the mass of the impactors), the ejecta accumulation rate depends only weakly on the sea-floor spreading rate, and the average will not differ significantly from the median. Given radiogenic heating rates at 3.85 Ga $c.\,3.4$ times higher than today, the heat flow would probably have been some 1.5–4 times higher than today, and thus sea-floor turnover times in the range of 6–45 Ma. The expected standing crop of basaltic and dunitic ejecta is between 70 and 400 m.

As a first approximation, we let all the ejecta react quickly, in effect consuming all the CO_2 for which there are cations (roughly 0.005 moles g^{-1} for basalt and 0.01 moles g^{-1} for ultramafic rocks; these values correct a propagating typo of Sleep & Zahnle (2001)). This yields from equation (18) an average CO_2 sink of $F_{ej} \approx 1 \times 10^{14}$ moles a^{-1}. This is large compared with all geological terms in the modern carbon cycle. Alternatively, we can regard the ejecta simply as additional reactable oceanic crust. New reactable oceanic crust was created at a rate of 1×10^{16} to 7.2×10^{16} g a^{-1}, presuming plate tectonics, global spreading rates of 7–48 km^2 a^{-1} (i.e. 2.3–16 times present), and a reactable depth of 500 m. These set upper limits on the hydrothermal CO_2 sink of 5×10^{13} to 3.6×10^{14} moles a^{-1}. These are comparable with the ejecta sink, but the latter is probably the more easily fully carbonatized, owing to the damaged and more mafic state of the ejecta. Under these assumptions it appears likely that reactions with ejecta will determine pCO_2.

A third, more ambitious, approach is to assume a mass distribution for the ejecta themselves and directly estimate the corresponding weathering rate using measured reaction rates of basaltic glasses. We have done this elsewhere (Sleep & Zahnle 2001); here we quote only the essential results corrected for typos. We described the cumulative mass distribution of the ejecta by a power law $N(>\mu) \propto \mu^{-\gamma}$, where μ is the fragment mass. We found that, for $\gamma < 1$, weathering goes as $pCO_2^{3-3\gamma}$; whereas for $\gamma \geq 1$, weathering is nearly independent of pCO_2. For $\gamma = 0.95$ we obtain

$$F_{ej} \approx 3 \times 10^{13} pCO_2^{0.15} \text{ moles a}^{-1} \qquad (19)$$

and for $\gamma \geq 1$ we obtain

$$F_{ej} \approx 5 \times 10^{13} \text{ moles a}^{-1} \qquad (20)$$

the latter being, to within a factor two, the same result we obtained above for immediate and complete reaction of ejecta.

Finally, we need an impact history. These are obtained from the lunar record, which itself is controversial. For our purposes it is not particularly important to choose sides in this debate. We arbitrarily assume a linear decline of the Hadean impact flux from an initially high value at 4.4 Ga to zero at 3.55 Ga, which yields a flux at 4.4 Ga closer to the lower end than to the upper end of estimates. There results

$$F_{ej} \approx 2 \times 10^{14} pCO_2^{0.15} \max(0, t - 3.7) \text{ moles a}^{-1} \qquad (21)$$

where time t is in Ga and the expression is tuned to give the appropriate impact flux at 3.85 Ga. The steep decline in the impact rate after 3.95 Ga is based on lunar data, although the specific cutoff date of 3.7 Ga is negotiable. Earlier behaviour is debatable. More aggressive extrapolations would imply greater impact flux in the more distant past, less atmospheric CO_2, and colder climates in early Hadean time than in our models.

An exemplary model

Figures 12–15 describe the CO_2 evolution of specific models indicated by the '⊕' symbol in Figures 7 & 8. These models feature a current mantle reservoir R_{man} of 1.44×10^{22} moles and a current ridge degassing flux $F_{ridge} = 2 \times 10^{12}$

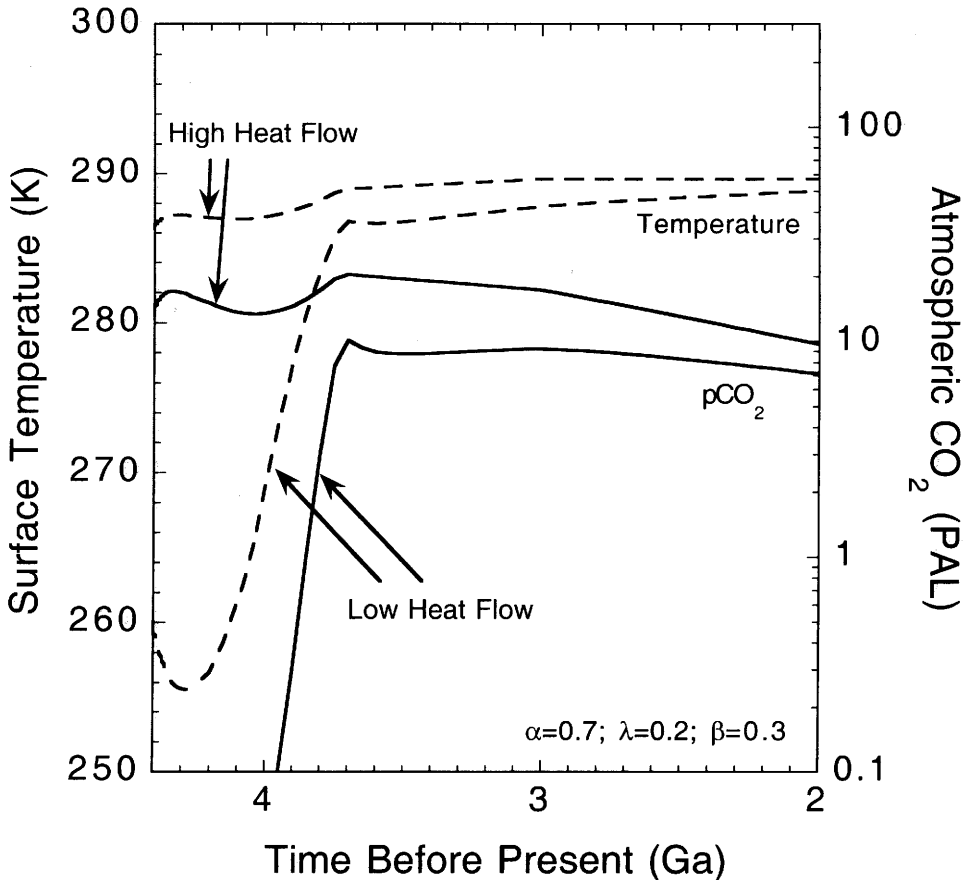**Fig. 12.** Temperature and pCO_2 histories for the specific models labelled '⊕' in Figures 7 and 8. These models use $\alpha = 0.7$, and $\beta = 0.3$. The last corresponds to some 250 ppm methane at 2.75 Ga. Results are shown with impact ejecta for low ($\mu = 0.2$) and high ($\mu = 0.7$) heat flow. In Hadean time the heat flow is important because sea floor and ejecta compete for CO_2; high heat flow implies high rates of CO_2 cycling through the upper mantle. With low rates of crustal creation the impact ejecta are an important sink on CO_2, which is driven to negligible levels.
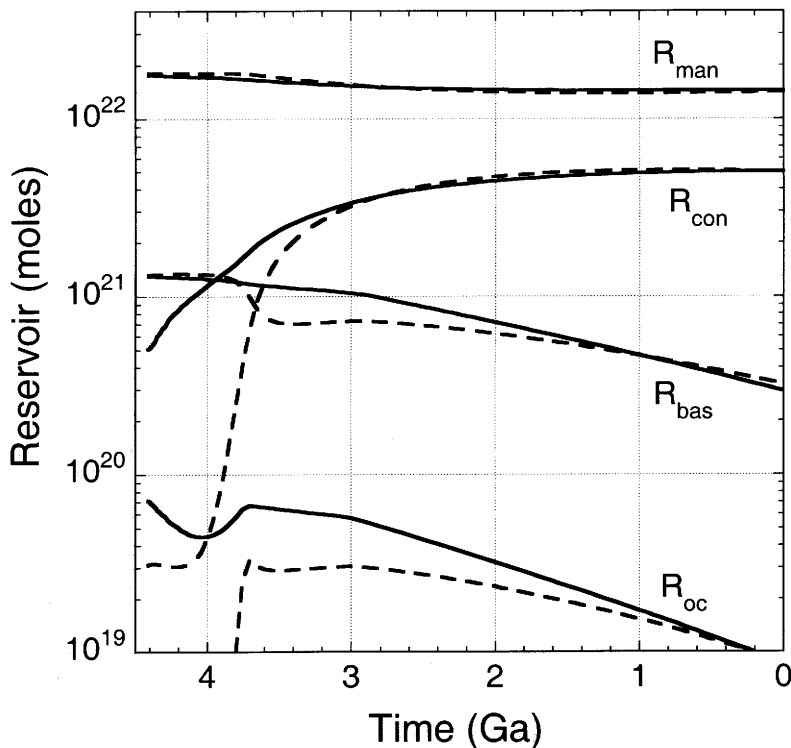
Fig. 13. Four important reservoirs of CO_2 are shown as functions of time for the models in Figure 12. High heat flow is denoted by continuous lines, low heat flow by dashed lines. Here we have chosen models in which the crustal reservoirs are initially constant in time; i.e. we have started from the equilibrium reservoirs. In particular, the equilibrium continental reservoirs are small and so these models begin with very little continental carbonate. The high heat-flow models churn the reservoirs fast enough that if we do not start at equilibrium values, the model quickly evolves to them, but in the low heat-flow models circulation is slow enough that the arbitrary initial conditions are remembered well into Archaean time. In general, the effect of abundant Hadean impact ejecta is to remove CO_2 from the continents and oceans and put it into the mantle.

moles a^{-1}. They use $\alpha = 0.7$, $\beta = 0.3$ and $\lambda = 0.2$ (i.e. 200 ppm CH_4 at 2.75 Ga) to illustrate two possible Earth histories. Continents are held constant. We make no special allowance for biological advances in chemical weathering. The most important nonstandard or nonuniformitarian feature of these models is that they assume a substantial methane greenhouse ($\lambda = 0.2$) all the way back. Without the additional greenhouse gas we expect a hard snowball Earth through most of Hadean time (because of large impact events even a snowball Hadean eon will stochastically enjoy temperate, tropical or hypertropical conditions) and all of Archaean time.

Figure 12 shows surface temperature and pCO_2 histories. These focus on Archaean and Hadean time. Results are shown for the different heat-flow histories. The models with ejecta weathering use equation (19). By construction these are

a warm model with relatively modest amounts of atmospheric CO_2. They implicitly depend on a large (biogenic?) methane source to maintain clement conditions. Without methane, ejecta weathering can easily drive surface temperatures below 240 K as we have shown elsewhere (Sleep & Zahnle 2001).

Figure 13 shows how the four major CO_2 reservoirs evolve in the $\oplus$ models. Because the models address Hadean time, they can be sensitive to the assumed initial conditions. Here we have arbitrarily chosen to present models in which the crustal reservoirs (R_{con} and R_{bas}) are initially in equilibrium with the sources and sinks. The high heat-flow models churn these reservoirs fast enough that the equilibrium sizes are quickly obtained whatever the initial choice is. But in low heat-flow models evolution is slow enough that the arbitrary initial conditions are
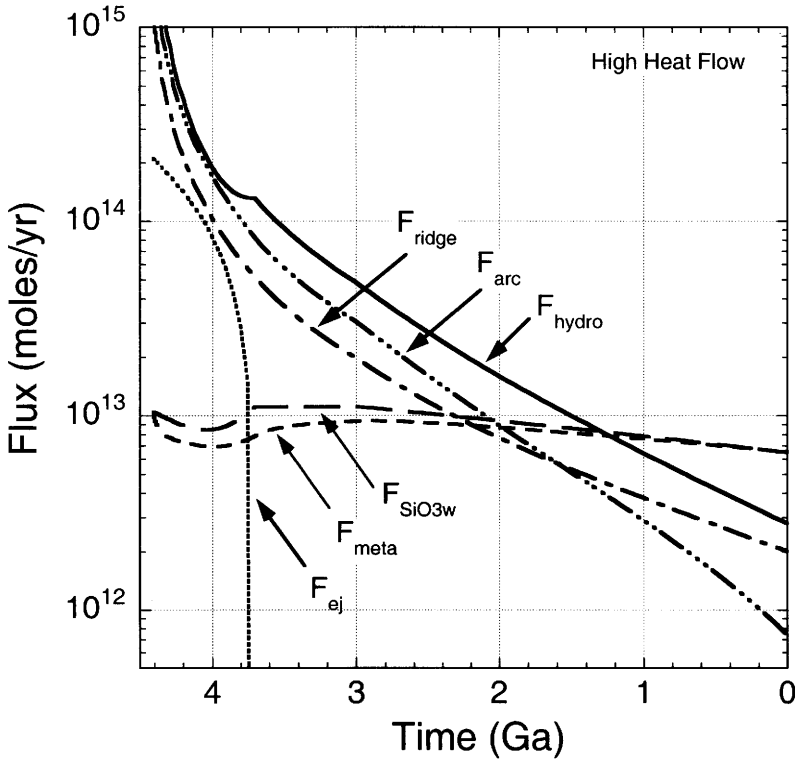
Fig. 14. Fluxes of CO_2 are shown as functions of time for the high heat-flow models in Figures 12 and 13. Impact ejecta are of minor importance compared with the rapid churning of the oceanic crust. In Archaean time, CO_2 is mostly controlled by processes involving the creation and subduction of oceanic crust. Continents become increasingly important through Proterozoic time, with the transition from mantle to continental control occurring at $c. 1.4\,\mathrm{Ga}$.

remembered well into Archaean time. In particular, in the low heat-flow $\oplus$ model shown here (dashed lines in Fig. 13), the equilibrium continental reservoir is initially very small. This is agreeable if one imagines that in the beginning CO_2 was begat by the Earth. But if instead the CO_2 arrived late or owing to very different environments on early Earth began mostly partitioned into surface reservoirs, as we expect would be the case if Earth cooled from a magma ocean (Sleep & Zahnle 2001; Sleep et al. 2001), it is possible that the early continental CO_2 reservoir was large and the low equilibrium value effectively unreachable. Both models predict that early in Earth's history $R_{bas} \approx 1.3 \times 10^{21}$ moles, equivalent to $c. 40\%$ carbonatization of the reactable upper 500 m oceanic basalt. The model requires 8% carbonatization today.

Figures 14 and 15 show the fluxes of CO_2 between reservoirs in the $\oplus$ models. Figure 14 addresses the high heat-flow ($\mu = 0.7$) $\oplus$ model. In these, the largest fluxes in Hadean time are associated with the oceanic cycle of crustal

creation and subduction; weathering of impact ejecta is of secondary importance. Thereafter the oceanic crustal cycle monotonically declines whereas the continental cycle of silicate weathering and metamorphism holds roughly constant with time whereas fluxes to and from the mantle decrease. (The continental cycle increases with time for $\alpha = 1$ (not shown).) The continental cycle becomes increasing important as time passes, as might be expected. The transition from mantle to continental control over the CO_2 cycle (here at $c. 1.4\,\mathrm{Ga}$) is a general feature of our models, although the timing varies.

It should be noted that the model predicts arc volcanic fluxes that are currently too low. This occurs because, in our model, the steady-state relation between the mid-ocean ridge flux and F_{arc} is $F_{arc}/F_{ridge} \approx (1 - C_{deep})/C_{deep}$. For $C_{deep} = 3/4$, the model predicts that the current arc volcanic flux should approach $F_{arc} \approx F_{ridge}/3 = 6.7 \times 10^{11}$ moles a^{-1} for $F_{ridge} = 2 \times 10^{12}$ moles a^{-1}. This is only marginally smaller than what we have assumed it would be without pelagic carbonates,
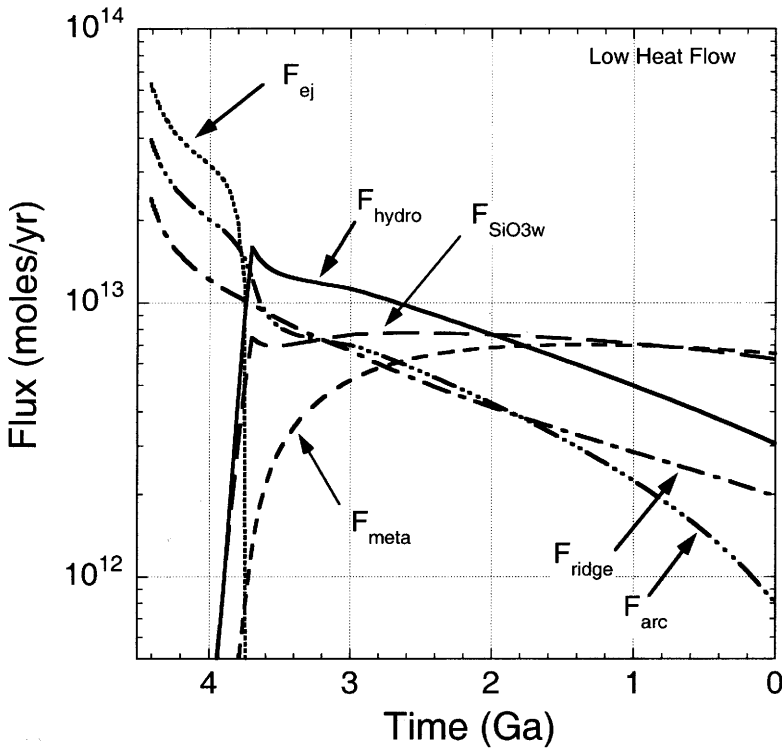
Fig. 15. Fluxes of CO_2 are shown as functions of time for the low heat-flow models shown in Figures 12 and 13. Impact ejecta dominate the CO_2 cycle in Hadean time. The oceanic crustal cycle controls CO_2 in Archaean time. Continents are important throughout Proterozoic time, with the transition from mantle to continental control occurring at $c.\,2.1$ Ga.

$(1 - C_{deep})F'_{sub} = 8.5 \times 10^{11}$ moles a^{-1}, but it is smaller than other estimates in the literature (see Marty & Tolstikhin 1998). To the extent that plumes contribute to the mantle's degassing, our estimate of the steady-state value of F_{arc} is raised proportionately.

Figure 15 addresses the low heat-flow ($\mu = 0.2$) ⊕ model. In this model impact ejecta completely dominate the Hadean CO_2 cycle. When impacts cease, control is passed to the oceanic crustal cycle, but continents become important fairly early and by $c.\,2$ Ga the continental cycle is the more important. The transition between oceanic and continental control is driven in part by mantle cooling and in part by decreasing heat flow. Overall, the transition between regimes is clear and its timing reasonable.

Conclusions, caveats and implications

It is well known that the crustal Urey cycle of silicate weathering and metamorphism can function as a dynamic buffer for atmospheric

pCO_2 and climate (Walker *et al.* 1981). Feedback is provided by the strong temperature dependence of silicate weathering. Less appreciated is that hydrothermal alteration of oceanic basalts can also function as a dynamic buffer on CO_2 (Sleep & Zahnle 2001). Feedback is provided by the dependence of carbonatization on dissolved carbonates in sea water. The Urey cycle links atmospheric CO_2 to continental carbonates and silicates; water serves as a catalyst, and the oceans and mantle are otherwise ignored. The oceanic cycle links surficial CO_2 to the mantle via subduction and outgassing at the mid-ocean ridges. Currently the continental cycle is more important, but earlier in Earth's history, especially if heat flow were higher than it is now, a warmer mantle would have made the oceanic cycles dominant. Oceanic control would have been greater still if continents were late to develop. The important feature of the oceanic cycle is that, although it can control CO_2, it does so without a thermostat. We infer that massive CO_2 greenhouses are implausible and that, if there were no other greenhouse gases

available to help, globally freezing temperatures are indicated for early Proterozoic and especially Archaean time.

In Hadean time huge amounts of mafic and ultramafic impact ejecta would probably have held atmospheric CO_2 levels strongly in check. This view of the Hadean Eon contrasts starkly with more traditional views in which significant ejecta and basaltic sinks are neglected and massive warm CO_2 atmospheres result (Morse & Mackenzie 1998). Despite its name, the Hadean Eon would have been the coldest era in the history of the Earth. Indeed, an ice-covered Earth has itself been recommended as an excellent environment for the origin of life (Bada et al. 1994).

Obviously models such as ours depend strongly on a wide range of poorly known parameters and debatable assumptions. It would not be fitting to claim any great certainty. To pick an example of how our models could fail, it could prove that Caldeira (1995) and Brady & Gíslason (1997) are right, and carbonatization of oceanic basalt proceeds at rates that depend little if at all on the sea-water CO_2 concentration. Readers can probably provide their own examples.

A possibly troubling feature of our models is that we implicitly predict a secular trend in the isotopic composition of carbonates. This would occur because the carbonate subducted would presumably have the isotopic composition of sea water, whereas CO_2 currently outgassed at mid-ocean ridges is isotopically lighter. One way to avoid this problem is to presume that carbonates and reduced carbon are subducted in the same proportions as they are produced. Because the mantle emits some reduced gases and subducts oxidized ferric iron (Lecuyer & Ricard 1999), some reductant must be subducted lest the continents grow secularly more reduced. The natural candidate, perhaps the only viable candidate, is reduced carbon, which is notably refractory and already known to be subducted. This is a reasonable expectation, and it is consistent with what is known of arc volcanoes today (see above), but it is unmotivated by our model.

Taking our conclusions at face value, there are two issues that need to be addressed. One issue is how our model breaks down at early times if carbonate subduction were inhibited by a hotter mantle. In our model the subduction of carbonatized oceanic crust closes the mantle's CO_2 cycle. Factors that inhibit carbonate subduction have the effect of stranding CO_2 in surface reservoirs. Although the capacity of the permeable layer of oceanic basalt to store CO_2 is large ($c.3 \times 10^{21}$ moles), it falls well short of the global

inventory of $c.2 \times 10^{22}$ moles of CO_2. In our models the sea floor's capacity is exceeded if C_{deep}, the fraction of subducted carbonate that reaches the mantle, becomes smaller than 20% (the modern value is between 64 and 84% (Fischer et al. 1998)). A massive CO_2 atmosphere could result if $C_{\text{deep}} < 0.2$. Surface temperatures exceeding 200°C are implied (Kasting & Ackerman 1986). We have addressed in more detail elsewhere (Sleep & Zahnle 2001; Sleep et al. 2001) what is required to make C_{deep} small, and how quickly the Earth might make the transition from uninhabitably hot to uncomfortably cold Hadean climates.

The other issue is the nature of, and implications of, a strong early greenhouse effect in which CO_2 is not the only player. Methane is the most plausible alternative because it is relatively stable and effective, and can easily be produced in the required amounts by modern levels of biogenic activity (Pavlov et al. 2000). But a methane greenhouse comes at an interesting price: large amounts of methane imply large amounts of irreversible hydrogen escape to space (Catling et al. 2001). At the limiting flux (Walker 1977), 100 ppm CH_4 implies an H_2 escape rate of 1.4×10^{12} moles a^{-1} and, if the methanogenesis ultimately derives from oxygenic photosynthesis (as it almost certainly must), a corresponding O_2 production rate of 7×10^{11} moles a^{-1}. This is about a tenth of the current rate at which O_2 is consumed by weathering (Walker 1977), but unlike weathering, global oxidation by hydrogen escape is unbalanced by reduction elsewhere. Eventually a methane greenhouse must oxidize the Earth (Catling et al. 2001).

References

ABBOTT, D. L., BURGESS, L., LONGHI, J. & SMITH, W. H. F. 1994. An empirical thermal history of the Earth's upper mantle. Journal of Geophysical Research, **99**, 13 835–13 850.

ALT, J. C. 1995. Subsurface processes in mid-ocean ridge hydrothermal systems. In: HUMPHRIS, S. E. ZIERENBERG, R. A. MULLINEAUX, L. S. & THOMSEN, R. E. (eds) Seafloor Hydrothermal Systems, Physical, Chemical, Biological, and Geological Interactions. Geophysical Monograph, American Geophysical Union, **91**, 85–114.

ALT, J. C. & TEAGLE, D. A. H. 1999. The uptake of carbon during alteration of oceanic crust. *Geochimica et Cosmochimica Acta*, **63**, 1527–1535.

ALT, J. C., MUEHLENBACHS, K. & HONNOREZ, J. 1986. An oxygen isotope profile through the upper kilometer of the oceanic crust, DSDP Hole 504B. *Earth and Planetary Science Letters*, **80**, 217–229.

ANBAR, A. D., ARNOLD, G. L., MOJZSIS, S. J. & ZAHNLE, K. J. 2001. Extraterrestrial iridium, sediment accumulation and the habitability of the early earth's surface. *Journal of Geophysical Research*, **106**, 3219–3236.

BADA, J. L., BIGHAM, C. & MILLER, S. L. 1994. Impact melting of frozen oceans on the early Earth Implications for the origin of life. *Proceedings of the National Academy of Sciences of the USA*, **91**, 1248–1250.

BERNER, R. A. 1994. 3GEOCARB II: A revised model of atmospheric CO_2 over Phanerozoic time. *American Journal of Science*, **294**, 56–91.

BERNER, R. A. 1997. The rise of plants and their effect on weathering and atmospheric CO_2, *Science*, **276**, 544–546.

BOWRING, S. A. & HOUSH, T. 1995. The Earth's early evolution. *Science*, **269**, 1535–1540.

BRADY, P. V. & GÍSLASON, S. R. 1997. Seafloor weathering controls on atmospheric CO_2 and global climate. *Geochimica et Cosmochimica Acta*, **61**, 965–973.

BRANTLEY, S. L. & KOEPENICK, K. W. 1995. Measured carbon dioxide emissions from Oldoiyo Lengai and the skewed distribution of passive volcanic fluxes. *Geology*, **23**, 933–936.

BUICK, R. & DUNLOP, J. S. R. 1990. Evaporitic sediments of early Archean age from the Warrawoona Group, North Pole, Western Australia. *Sedimentology*, **37**, 247–277.

CALDEIRA, K. 1995. Long term control of atmospheric carbon: low-temperature seafloor alteration or terrestrial silicate-rock weathering? *American Journal of Science*, **295**, 1077–1114.

CALDEIRA, K. & KASTING, J. F. 1992. The life span of the biosphere revisited. *Nature*, **360**, 721–723.

CATLING, D. C., ZAHNLE, K. & MCKAY, C. P. 2001. Biogenic methane, hydrogen escape, and the irreversible oxidation of the early Earth. *Science*, **293**, 839–843.

CATUBIG, N. R., ARCHER, D. E., FRANÇOIS, R., DEMENOCAL, P., HOWARD, W. & YU, E.-F. 1998. Global deep-sea burial rate of calcium carbonate during the last glacial maximum, *Paleoceanography*, **13**, 298–310.

DESMARAIS, D. J. & MOORE, J. G. 1984. Carbon and its isotopes in mid-oceanic basaltic glasses. *Earth and Planetary Science Letters*, **69**, 43–57.

EKART, D. D., CERLING, T. E., MONTAÑEZ, I. P. & TABOR, N. J. 1999. A 400 million year carbon isotopic record of pedogenic carbonate: implications for paleoatmospheric carbon dioxide. *American Journal of Science*, **299**, 805–827.

FISCHER, T. P., GIGGENBACH, W. F., SANO, Y. & WILLIAMS, S. N. 1998. Fluxes and source of volatiles

dischanged from Kudryavy, a subduction zone volcano, Kurile Islands. *Earth and Planetary Science Letters*, **160**, 81–96.

FRANCK, S., KOSSACKI, K. & BOUNAMA, C. 1999. Modelling the global carbon cycle for the past and future evolution of the earth system. *Chemical Geology*, **159**, 305–317.

FRANÇOIS, L. M. & WALKER, J. C. G. 1992. Modelling the Phanerozoic carbon cycle and climate: constraints from the $^{87}Sr/^{86}Sr$ isotopic ratio of sea water. *American Journal of Science*, **292**, 81–135.

GERLACH, T. M. 1991. Present-day CO_2 emission from volcanoes. *EOS Transactions, American Geophysical Union*, **72**, 249–251.

GODDÉRIS, Y. & FRANÇOIS, L. M. 1995. The Cenozoic evolution of the strontium and carbon cycles: relative importance of continental erosion and mantle exchanging. *Chemical Geology*, **126**, 167–190.

GROTZINGER, J. P. & KASTING, J. F. 1993. New constraints on Precambrian ocean composition. *Journal of Geology*, **101**, 235–243.

HOLLAND, H. D. 1978. *The Chemistry of the Atmosphere and Oceans*. Wiley, New York.

HOLLAND, H. D. 1984. *The Chemical Evolution of the Atmosphere and Ocean*. Princeton University Press, PRINCETON, NJ.

HOOFT, E. E. E., SCHOUTEN, H. & DETRICK, R. S. 1996. Constraining crustal emplacement processes from the variation in seismic layer 2A thickness at the East Pacific Rise. *Earth and Planetary Science Letters*, **142**, 289–309.

KADKO, D., BAROSS, J. & ALT, J. 1995. The magnitude and global implications of hydrothermal flux. *In*: HUMPHRIS, S. E., ZIERENBERG, R. A., MULLINEAUX, L. S. & THOMSEN, R. E. (eds) *Seafloor Hydrothermal Systems, Physical, Chemical, Biological, and Geological Interactions*. Geophysical Monograph, American Geophysical Union, **91**, 446–466.

KASTING, J. F. & ACKERMAN, T. P. 1986. Climatic consequence of very high carbon dioxide levels in the early Earth's atmosphere, *Science*, **234**, 1383–1385.

KEMPE, S. & DEGENS, E. T. 1985. An early soda ocean? *Chemical Geology*, **53**, 95–108.

KEMPE, S. & KAZMIERCZAK, J. 1994. The role of alkalinity in the evolution of ocean chemistry, organization of living systems, and biocalcification processes. *Bulletin de l'Institut océanographique, Monoco, numéro spécial*, **13**, 61–117.

KERRICK, D. M. & CONNOLLY, J. A. D. 2001. Metamorphic devolatization of subducted oceanic metabasalts: implications for seismicity, arc magmatism and volatile recycling. *Earth and Planetary Science Letters*, **189**, 19–29.

KIEHL, J. T. & DICKINSON, R. E. 1987. A study of the radiative effects of enhanced atmospheric CO_2 and CH_4 on early Earth surface temperatures. *Journal of Geophysical Research*, **92**, 2991–2998.

KOSTER VAN GROOS, A. F. 1987. Weathering, the carbon cycle, and differentiation of the continental crust and mantle. *Journal of Geophysical Research*, **93**, 8952–8958.

LANGMUIR, C. H., KLEIN, E. M. & PLANK, T. 1992. Petrological systematics of mid-ocean ridge basalts: constraints on melt generation beneath ridges. *In*: PHIPPS MORGAN, J., BLACKMAN, D. K. & SINTON, J. M. (eds) *Mantle Flow and Melt Generation of Mid-ocean Ridges*. Geophysical Monograph, American Geophysical Union, **71**, 183–280.

LASAGA, A. C., BERNER, R. A. & GARRELS, R. M. 1985. An improved geochemical model of atmospheric CO_2 fluctuations over the past 100 million years. *In*: SUNDQUIST, E. T. & BROECKER, W. S. (eds) *The Carbon Cycle and Atmospheric CO_2: Natural Variations Archean to Present*. Geophysical Monograph, American Geophysical Union, **32**, 397–411.

LÉCUYER, C. & RICARD, Y. 1999. Long-term fluxes and budget of ferric iron: implication for the redox state of the Earth's mantle and atmosphere. *Earth and Planetary Science Letters*, **165**, 197–211.

MACLOED, G., MCKEOWN, C., HALL, A. J. & RUSSELL, M. J. 1994. Hydrothermal and ocean pH conditions of possible origin of life. *Origins of Life and Evolution of the Biosphere*, **24**, 19–41.

MARTY, B. & JAMBON, A. 1987. $C/^3He$ in volatile fluxes from the solid Earth: implications for carbon geodynamics. *Earth and Planetary Science Letters*, **83**, 16–26.

MARTY, B. & TOLSTIKHIN, I. N. 1998. CO_2 fluxes from mid-oceanic ridges, arcs, and plumes. *Chemical Geology*, **145**, 233–248.

MOJCZIS, S. J., HARRISON, T. M. & PIDGEON, R. T. 2001. Oxygen-isotope evidence from ancient zircons for liquid water at the Earth's surface 4300 Myr ago. *Nature*, **409**, 178–181.

MORSE, J. W. & MACKENZIE, F. T. 1998. Hadean ocean carbonate geochemistry. *Aquatic Geochemistry*, **4**, 301–319.

OWEN, T., CASS, R. D. & RAMANATHAN, V. 1979. Enhanced CO_2 greenhouse to compensate for reduced solar luminosity on early Earth. *Nature*, **277**, 640–642.

PAVLOV, A. A., KASTING, J. F., BROWN, L. L., RAGES, K. A. & FREEDMAN, R. 2000. Greenhouse warming by CH_4 in the atmosphere of early Earth, *Journal of Geophysical Research*, **105**, 11 981–11 990.

PLANK, T. & LANGMUIR, C. H. 1998. The chemical composition of subducting sediment and its consequences for the crust and mantle. *Chemical Geology*, **145**, 325–394.

RINGWOOD, A. E. 1961. Changes in solar luminosity and some possible terrestrial consequences. *Geochimica et Cosmochimica Acta*, **21**, 295–296.

RUSSELL, M. J. & HALL, A. J. 1997. The emergence of life from iron monosulphide bubbles at a submarine hydrothermal redox and pH front. *Journal of the Geological Society, London*, **154**, 377–402.

RYE, R., KUO, P. H. & HOLLAND, H. D. 1995. Atmospheric carbon dioxide concentrations before 2.2 billion years ago. *Nature*, **378**, 603–605.

SAGAN, C. & MULLEN, G. 1972. Earth and Mars: evolution of atmospheres and surface temperatures. *Science*, **177**, 52–56.

SANO, Y. & WILLIAMS, S. N. 1996. Fluxes of mantle and subducted carbon along convergent plate boundaries. *Geophysical Research Letters*, **23**, 2749–2752.

SANSONE, F. J., MOTTL, M. J., OLSON, E. J., WHEAT, C. G. & LILLEY, M. D. 1998. CO_2-depleted fluids from mid-ocean ridge-flank hydrothermal springs. *Geochimica et Cosmochimica Acta*, **62**, 2247–2252.

SCHMIDT, R. M. & HOUSEN, K. R. 1987. Some recent advances in the scaling of impact and explosion cratering. *International Journal of Impact Mechanics*, **5**, 543–560.

SCHULTZ, A. & ELDERFIELD, H. 1997. Controls on the physics and chemistry of seafloor hydrothermal circulation. *Philosophical Transactions of the Royal Society of London, Series A*, **355**, 387–425.

SCHULTZ, A. & ELDERFIELD, H. 1999. Controls on the physics and chemistry of seafloor hydrothemal circulation. *In*: CANN, J. R., ELDERFIELD, H. & LAUGHTON, A. (eds) *Mid-ocean Ridges, Dynamics of Processes Associated with Creation of New Oceanic Crust*. Cambridge University Press, Cambridge, 171–209.

SCHWARTZMAN, D. & MCMENAMIN, M. 1993. A much warmer Earth surface for most of geologic time: Implications to biotic weathering. *Chemical Geology*, **107**, 221–223.

SCHWARTZMAN, D. & VOLK, T. 1989. Biotic enhancement of weathering and the habitability of Earth. *Nature*, **340**, 457–460.

SCHWARTZMAN, D. & VOLK, T. 1991. Biotic enhancement of weathering and surface temperatures on earth since the origin of life. *Paleogeography, Paleoclimatology, Paleoecology*, **90**, 357–371.

SIBLEY, D. F. & VOGEL, T. A. 1976. Chemical mass balance of the Earth's crust: the calcium dilemma and the role of pelagic sediments. *Science*, **192**, 551–553.

SLEEP, N. H. 1979. Thermal history and degassing of the earth: some simple calculations. *Journal of Geology*, **87**, 671–686.

SLEEP, N. H. & ZAHNLE, K. 2001. Carbon dioxide cycling and implications for climate on ancient Earth. *Journal of Geophysical Research*, **106**, 1373–1399.

SLEEP, N. H., ZAHNLE, K. & NEUHOFF, P. S. 2001. Initiation of clement surface conditions on the earliest Earth. *Proceedings of the National Academy of Sciences*, **98**, 3666–3672.

STAUDIGEL, H., HART, S. R., SCHMINCKE, H.-U. & SMITH, B. M. 1989. Cretaceous ocean crust at DSDP sites 417 and 418: carbon uptake from weathering versus loss by magmatic outgassing. *Geochimica et Cosmochimica Acta*, **53**, 3091–3094.

STAUDIGEL, H., PLANK, T., WHITE, B. & SCHMINCKE, H.-U. 1996. Geochemical fluxes during seafloor alteration of basaltic upper oceanic crust: DSDP sites 417 and 418. *In*: BEBOUT, G. E., SCHOOL, D. W., KIRBY, S. H. & PLATT, J. P. (eds) *Subduction Top to Bottom*. Geophysical Monograph, American Geophysical Union, **96**, 19–36.

STEIN, C. A., STEIN, S. & PELAYO, A. M. 1995. Heat flow and hydrothermal circulation. *In*: HUMPHRIS, S. E., ZIERENBERG, R. A., MULLINEAUX, L. S. & THOMSEN, R. E. (eds) *Seafloor Hydrothermal*

Systems, Physical, Chemical, Biological, and Geological Interactions. Geophysical Monograph, American Geophysical Union, **91**, 425–445.

TAJIKA, E. & MATSUI, T. 1992. Evolution of terrestrial proto-CO_2 atmosphere coupled with thermal history of the Earth. *Earth and Planetary Science Letters*, **113**, 251–266.

TAJIKA, E. & MATSUI, T. 1993. Evolution of seafloor spreading rate based on 40Ar degassing history. *Geophysical Research Letters*, **20**, 251–266.

WALKER, J. C. G. 1977. *Evolution of the Atmosphere.* Macmillan, New York.

WALKER, J. C. G. 1985. Carbon dioxide on the early Earth. *Origins of Life and Evolution of the Biosphere*, **16**, 117–127.

WALKER, J. C. G., HAYS, P. B. & KASTING, J. F. 1981. A negative feedback mechanism for the long-term stabilization of the Earth's surface temperature. *Journal of Geophysical Research*, **86**, 9776–9782.

WEDEPOHL, K. H. 1995. The composition of the continental crust. *Geochimica et Cosmochimica Acta*, **59**, 1217–1232.

WILDE, S. A., VALLEY, J. W., PECK, W. H. & GRAHAM, C. M. 2001. Evidence from detrital zircons for the existence of continental crust and oceans on the Earth 4.4 Gyr ago. *Nature*, **409**, 175–178.

WILKINSON, B. H. & WALKER, J. C. G. 1989. Phanerozoic cycling of sedimentary carbonate. *American Journal of Science*, **289**, 525–548.

ZAHNLE, K. & SLEEP, N. H. 1996. Impacts and the early evolution of life. *In*: THOMAS, P. J., CHYBA, C. F. & McKAY, C. P. (eds) *Comets and the Origin and Evolution of Life*, 175–208.

ZHANG, Y. & ZINDLER, A. 1993. Distribution and evolution of carbon and nitrogen in Earth. *Earth and Planetary Science Letters*, **117**, 331–345.